

**Spontaneously Formed Higher-Order Architectures of
Amphiphilic Polypeptides with Other Components**

Md. Mofizur Rahman

2019

CONTENTS

Contents	iii
List of Abbreviations	iv
List of the Measurement Instruments Used in the Present Thesis	v
Chapter 1 General Introduction	1
Chapter 2 Spontaneous Formation of Gating Lipid Domain in Uniform-Size Peptide Vesicles for Controlled Release	21
Chapter 3 Tubular network composed of a mixture of amphiphilic polypeptides having different hydrophilic blocks	49
Chapter 4 Concluding Remark	65
List of Publications	69
Acknowledgement	71

List of Abbreviations

¹ H NMR	Proton Nuclear Magnetic Resonance spectroscopy
Boc	<i>tert</i> -butyloxycarbonyl
CD	Circular Dichroism
Cryo-TEM	Cryogenic Transmission Electron Microscopy
DCC	Dicyclohexylcarbodiimide
DIEA	<i>N,N</i> -Diisopropylethylamine
DLS	Dynamic Light Scattering
DMF	<i>N,N</i> -Dimethylformamide
DPPC	Dipalmitoylphosphatidylcholine
DSC	Differential Scanning Calorimetry
ED	Electron Diffraction
EtOH	Ethanol
FITC	Fluorescein isothiocyanate
FT-IR/ATR	Fourier Transform Infrared spectroscopy/Attenuated Total Reflection
GA	Glucosamino Acid
HATU	<i>O</i> -(7-azabenzotriazol-1-yl)-1,1,3,3-tetramethyluronium hexafluorophosphate
HOBt	1-hydroxybenzotriazole
MALDI-TOF	Matrix-Assisted Laser Desorption Ionization Time of Flight
MeOH	Methanol
MS	Mass Spectroscopy
NBD-PE	1,2-distearoyl- <i>sn</i> -glycero-3-phosphoethanolamine- <i>N</i> -(7-nitro-2-1,3-benzoxadiazol-4-yl) (ammonium salt)
Rho-PE	1,2-dipalmitoyl- <i>sn</i> -glycero-3-phosphoethanolamine- <i>N</i> -(lissamine rhodamine B sulfonyl) (ammonium salt)
TEM	Transmission Electron Microscopy
TFA	Trifluoroacetic Acid
TLC	Thin Layer Chromatography

List of the Measurement Instruments Used in the Present Thesis

^1H NMR	Bruker DPX-400 spectrometer
CD	JASCO J-600 CD spectropolarimeter
DLS	Photal Otsuka DLS-8000
DSC	DSC 7000X, Hitachi
FAB MS	JEOL HA110 spectrometer
Fluorometer	JASCO FP-6500 spectro fluorometer
FT-IR/ATR	Nicolet 6700 FT-IR spectrometer
MALDI-TOF MS	JEOL JMS-ELITE spectrometer Bruker ultraflex III mass spectrometer
Optical and fluorescence microscope	Olympus IX70 Keyence VHX-1000
TEM	JEOL JEM-2000EXII instrument
UV	JASCO V-550 spectrophotometer

Chapter 1

General Introduction

1. Introduction

It undergoes a spontaneous predefined self-assembly process with specific directionality, adjustable, reversible noncovalent interactions such as electrostatic force, hydrogen bonding, aromatic π - π stacking, metal chelation, van der Waals interaction etc. Rational design of minimal molecular building blocks. The most interesting aspect of supramolecular assembly is the dynamic nature of noncovalent bonds. This makes them adaptive and creates nanostructures with self-healing and stimuli-responsive nature. In addition, supramolecular interactions are the basis for the structure and function of all biological systems. Including formation of cell membranes from simple hydrophobic interactions between amphipathic phospholipid molecules, DNA double helix formation by specific hydrogen bond interactions between nucleobases, and complex protein folding into exact tertiary structure. There are many examples of simple to complicated supramolecular aggregates in biological systems. Quaternary structure from the polypeptide chain. Using nature as a source of inspiration, many synthetic supramolecular nanomaterials are formed by specific noncovalent folding of macromolecules by repetitive interactions between reasonably designed small molecule building blocks (eg , Folded over) or a combination of both.¹⁻⁴

Naturally occurring and robust self-associating amyloid fibril aggregates promoted the use of peptides as biomimetic supramolecular structural motifs in nanotechnology. Over the years, peptides have proven to be excellent structural units for creating more complex supramolecular structures and functions. In contrast to other structural building blocks, peptides have many unique and desirable properties for biotechnological applications, such as biocompatibility, sequence specific secondary structure, chemical diversity, biomolecular recognition and ease of synthesis. In addition, peptide supramolecular assemblies exhibit abundant diversity in nano- and microstructures including hydrogels, fibers, tubes, rods, films, plates, nanocages, vesicles and the like. The dynamic nature of the peptide aggregation allows spatial and temporal control over the final product structure.⁵ In addition, control over peptide supramolecular organization was achieved by adding external stimuli such as pH, temperature, chemicals, enzymes, solvents, magnetic fields and electric fields. These stimuli further uniquely serve to alter the properties and characteristics of the peptide nano-

assembly. In addition, because peptide aggregates exhibit diverse physicochemical properties, they can be used in a variety of energy storage devices, displays and light-emitting devices, ferroelectric and piezoelectric components, superhydrophobic surfaces for self-cleaning applications, Materials science and biological applications are explored. Inorganic superstructure scaffold, organometallic framework, ultra-sensitive sensor, 3D hydrogel scaffold for tissue engineering, drug delivery etc.⁵⁻¹⁷

2. Polypeptide Having α -Helix

Not only did several studies focused on α helix peptides that had been done over the past quarter century contributed to a better understanding of protein folding into the native biologically active conformation, very interesting in the design of therapeutic drugs. It is effective for treating diseases related to interruption of protein-protein interaction. Since the early 1990's, numerous experimental data on the folding and stability of α -helices in monomeric peptides have been accumulated. These data demonstrate that the amino acid sequence of the α -helix is not optimal to normally ensure high conformational stability. This can be an important factor in preventing the accumulation of erroneous intermediate products in the folding of globular proteins. Therefore, designing short α -helical peptides and proteins with enough conformational stability under specific ambient conditions (temperature, pH, and ionic strength) is still an interesting problem of practical importance in protein engineering. A huge number of experimental data on physical interactions affecting the stability of α helix in proteins and monomeric peptides allows researchers to build a theoretical model describing α helix - coil transitions and design them using them we can create a new high efficiency calculation for. A helix peptide characterized by high conformational stability. Stabilization of α -helices has been used repeatedly to design industrially relevant enzymes that can act at high temperatures. In this review, we use amino acids with increased tendency towards α -helical conformation, including molecular mechanisms such as alteration of amino acid composition of proteins in thermophilic organisms, insertion of additional ion pairs and hydrogen bonds, formation of disulfide bridges, enhancement of hydrophobic interactions, introduction of proline substitution into the loop, binding to metal ions, denser packing and the like.¹⁸⁻²⁵

General Introduction

Beginning in the late 1980's and especially in the 1990's a number of experiments were conducted in which amino acid substitutions in short synthetic polyalanine based peptides were used to study various interactions in α -helices. With this approach, researchers could accumulate enough data and be able to proceed quantitatively to the cooperative mechanism of conformational transfer to the α helix conformation for peptides with random sequences. Currently, it is believed that each of the 20 natural amino acids has an intrinsic tendency in peptides and proteins to form α -helix structures related to their covalent structure (eg, the configuration of side chains of amino acids changes in entropy transition from random conformation to α -helix). Furthermore, the stability of conformation of α -helix protein is due to the interaction between side chains (between residues at positions i , $i + 3$ and i , $i + 4$) (electrostatic between charged polar residues the interaction) is affected. Capping interactions between α -helical macro dipoles, as well as residues adjacent to the α -helix in the backbone of the protein in the α and helix turns and unbound NH- and CO- moieties. Furthermore, a local motif of amino acid sequence containing residues adjacent to α -helix. It is specifically packed or forms a network to the residues of the first (N-terminal) and the last (C-terminal) turn of the helix. It has also been reported to have specific hydrogen bonds with it. Normally, the structural tendency of amino acids is believed to be independent of their position in the α helix. However, the first and last turns of the α -helix are not equivalent to the rest of the helix.²⁶⁻

34



Figure 1. The accuracy of the theoretical models of α -helix/random coil transitions in the description of experimental findings on measuring the stability of α -helical peptides with complex amino acid sequences is significantly reduced if no allowance is made for this factor.

The amino acid sequences of membrane-bound α -helices fall into two general categories. Mainly hydrophobic α -helices tend to straddle the membrane, generally in a direction perpendicular or nearly perpendicular to the surface of the bilayer. The central core of these molecules consists exclusively of lipophilic amino acid residues such as leucine, valine and phenylalanine, but there are specific examples where there are a few polar residues in the TM domain (such as MHC class II invariant chain). These residues often play an important role in stabilizing the functional oligomer complex via the formation of helix-to-helix hydrogen bonds. The N-terminus and the C-terminus of the TM α helix are near the polar / charged lipid headgroups, and more likely polar or charged amino acids are likely to be found at these positions. Studies of transmembrane α helices also reveal that positively charged residues such as Lys and Arg are excessively present in the lipid-cytoplasmic interface region of the cell membrane, compared to negatively charged residues. Stability and orientation of the helix in the membrane.³⁷

This "positive inside rule" hypothesis is often used for peptide design, identification of transmembrane regions, and prediction of membrane protein topology. Thus, peptides which comprise a hydrophobic core and which adopt an α -helical structure with polar and / or charged (especially positively charged) residues at the ends are more likely to spontaneously be inserted into the cell membrane (Figure. 2a)

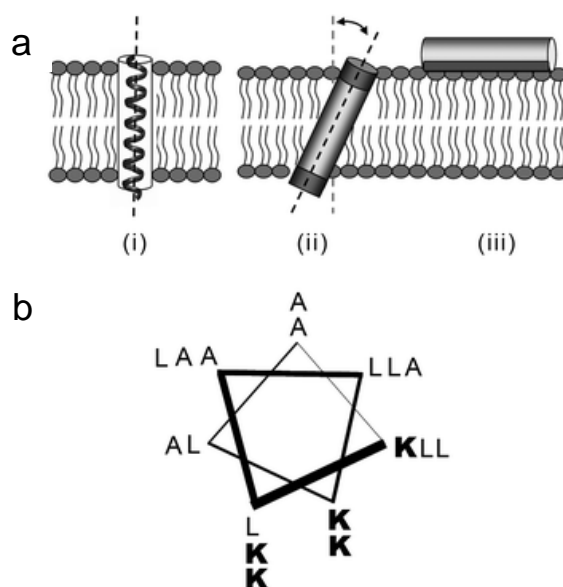


Figure 2. Sequence requirements for membrane association (a) Depending on the thickness of the membrane and the length of the transmembrane sequence, the transmembrane helix can extend the lipid membrane perpendicular to the membrane plane (i) or " It is forced to "tilt" (ii). Hydrophobic amino acid group in the bilayer nonpolar core. Spiral peptides that are likely to insert spontaneously into the bilayer are those with a hydrophobic core (light gray) and polar and / or charged ends (dark gray). (Iii) The amphiphilic helix has a sequence that results in helical polar (dark gray) and nonpolar (light gray) planes, which allows interaction with both head groups and lipid chains. (B) Helical wheel representation of amphiphilic α -helical model peptide MAP. Indicate how polar Lys residues (in bold) all fall on one side of the spiral and the remaining helices are nonpolar.

The length of the helix may also affect the ability to insert into the lipid membrane. Because the cell membrane has a hydrophobic core in the range of about 0.2 - 0.3 nm, 7, 10, the membrane spanning the α - helix contains a hydrophobic region consisting of about 15 - 20 residues. Due to variations in the chain length of different lipids (resulting in membranes of varying thickness), the α -helix is completely substituted for the bilayer normal to accommodate all the hydrophobic amino acids in the hydrophobic amino acid You need to "tilt" from a vertical position. The area of the membrane (Figure 2a). Therefore, the helical inclination angle varies depending on the length of the lipid chain and becomes more prominent in shorter lipid chains (ie, thinner membranes). In contrast, the

amphipathic α -helix has a sequence consisting of both polar and a polar residue throughout the helix. However, the arrangement of these residues results in helical polar and nonpolar "planes" as shown in Figure 2a (iii). The amphipathic α -helical model peptide MAP, eg 11, forms an α -helix from the repeating sequence of Leu, Ala and Lys residues, resulting in a polar helical plane and a nonpolar plane (Figure 2 b). These separate aspects allow amphipathic helices to interact simultaneously with aqueous extracellular and cytoplasmic environments as well as polar lipid head groups, as well as the hydrophobic core of the membrane. As these properties suggest, amphipathic α -helices can associate with membranes via various mechanisms. They can bind to the surface of the membrane (Figure 2a (iii))^{39,40} and possibly later into the membrane.

3. Amphiphilic Polypeptide Assemblies

Here, we focus on polypeptide amphiphiles, which assembly to form stable complexes owing to numerous inter- and intra-interactions, including van der Waals forces, H-bonding, π - π stacking, dipole moments, disulfide bonding, electrostatic interactions, concavo-convex and steric interactions. The polypeptide assemblies show lipid-like membrane fluidity, morphological diversity and biocompatibility. In addition, it has recently been shown that polypeptide assemblies can create a Janus soft matter consisting of a phase-separated membrane by integration. Using these unique properties, attempts were made to use these polypeptide assemblies for biomedical applications, including bio-matrices, carriers of drug delivery systems and in vivo imaging.

In this chapter, as shown in Figure 3, we show the assemblies of amphiphilic polypeptides and derivatives with polyethylene glycol (PEG), and composite formation by integration with other components such as lipids or cholesterol.

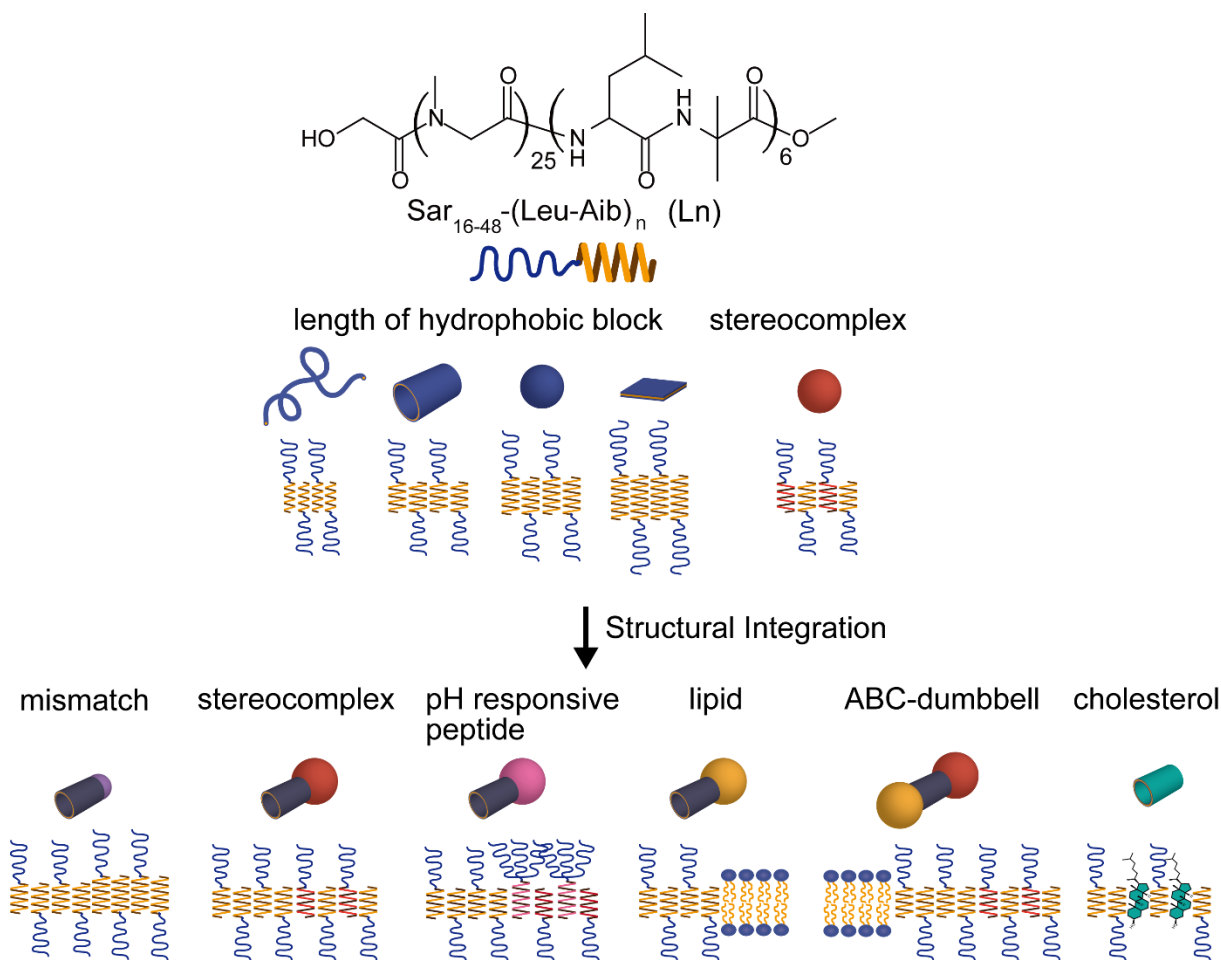


Figure 3. Amphiphilic polypeptide assemblies with other components.

Ueda and coworkers have reported some unique morphologies prepared from polypeptide amphiphiles⁴³⁻⁴⁸. These amphiphiles have an α -helical forming peptide as a hydrophobic block. An α -helical hydrophobic block is rigid and uniform shape due to the intramolecular hydrogen bonding, resulting that it can enable to form stable assemblies, have lateral fluidity without entangling between hydrophobic blocks and make it easy to control the

shape of assembly. Hydrophilic block is composed of poly(sarcosine). Poly(sarcosine) forms polymer brush on the surface of assembly and shows the similar hydrophilicity and stealth ability to polyethylene glycol. In addition, poly(sarcosine) is biodegradable and not toxic in a body, resulting that poly(sarcosine) is very useful tool as a biomaterial for medical application. Furthermore, in previous reports, he also reported that a mixture of two enantiomeric amphiphilic polypeptides with a right- and a left-handed helical block self-assemble to form large planar and curved sheets. The sheets could be converted to a round-bottom flask-type molecular assembly upon heating in buffer, where the neck part was composed of a single component and the sphere part composed of the stereocomplex.^{44,45}

3.1 Length of Hydrophobic Chain

The morphologies of assemblies can be controlled by the design of amphiphilic polypeptides. The design refers to the character of the hydrophilic block and the hydrophobic block and the valence of each block type. In particular, the hydrophobic block is one of the most important blocks to control the shape because the molecular orientation of packed amphiphiles depends on the character of the hydrophobic block. Here, we synthesized some amphiphilic polypeptides with the hydrophilic polypeptide polysarcosine (Sar)_n and various lengths of a hydrophobic helix block composed of L-leucine (L-Leu) and 2-aminoisobutyryl (Aib); (Sar)₁₆-*b*-(L-Leu-Aib)₄ (L8), (Sar)₂₅-*b*-(L-Leu-Aib)₆ (L12), (Sar)₂₆-*b*-(L-Leu-Aib)₇ (L14), (Sar)₃₂-*b*-(L-Leu-Aib)₈ (L16), (Sar)₄₀-*b*-(L-Leu-Aib)₉ (L18) and (Sar)₄₈-*b*-(L-Leu-Aib)₁₀ (L20). According to the Griffin hydrophilic-lipophilic balance (HLB)⁴⁹⁻⁵¹, these polypeptides have similar values of 12.0–13.0. There is no significant difference among these hydrophilic-lipophilic balances. However, these polypeptides assembly to form different shapes in aqueous solvent.

These assemblies were categorized into two groups. One group is the fiber-shaped assembly of L8 (Figure 4a) and the other group is the sheet-shaped assembly of L12–L20.

General Introduction

Circular dichroism spectra demonstrated that the hydrophobic block of L8 formed a 3_{10} -helix and others forming an α -helix (Figure 4e). The packing of α -helices is known to form planer sheets because the α -helix has a thicker diameter than the 3_{10} -helix. Thus, the critical packing parameter⁵² of L8 was different from the other amphiphiles. The reason why L8 formed a fiber-shaped assembly is due to the difference of the helix structure.

We also found another difference among the assemblies of L12–L20. When these sheet assemblies were heated at 90 °C, L12 and L14 sheets rolled up to form a tubular assembly (Figure 4b)^{38,53}, the L16 sheet transformed into a vesicular assembly (Figure 4c)⁴⁴, and L18 and L20 sheets maintained their shapes (Figure 4d). The edge of sheets is considered to be hydrophobic, and sheets tend to roll up to decrease the area of the edge. L12–L16 species were considered to not have sufficient lengths of hydrophilic chains to maintain the planar sheet shape during heating. On the other hand, L18 and L20 have sufficient lengths of the hydrophilic chain to cover the hydrophobic edge of the sheet. As a result, L18 and L20 sheets were stable and did not change shape during heating.

The formations of tubes of L12 and L14, and the sphere formed by L16 were most likely due to the difference of concavo-convexo interactions between neighboring helices. The anisotropic nature of L12 and L14 membranes facilitated tube formation. However, L16 was too long to be packed with a tilt angle; thus, L16 packed in a parallel manner to form an isotropic sphere.

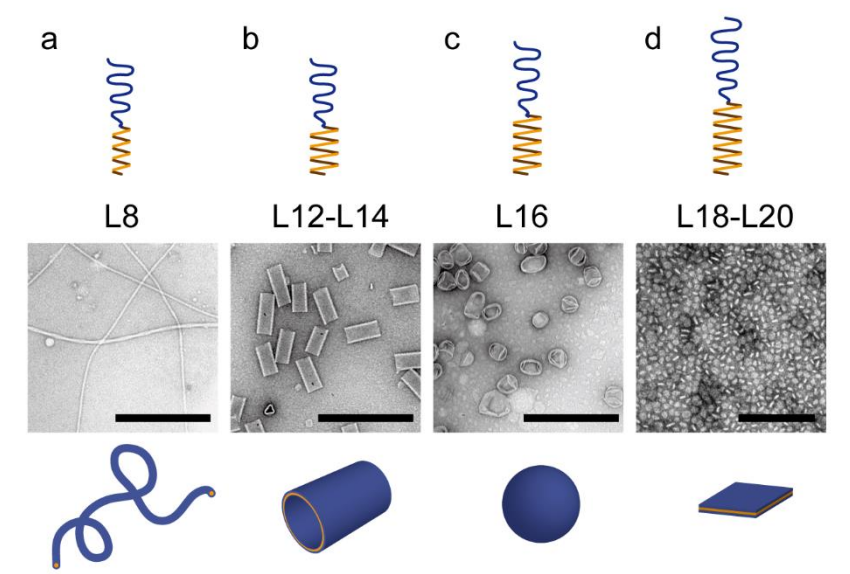


Figure 4. Schematic illustration and negative staining images by a transmission electron microscope (TEM). The assemblies were composed of a single component of an amphiphilic polypeptide with various lengths of the hydrophobic block: $(\text{Sar})_{16-48}\text{-}b\text{-(L-Leu-Aib)}_n$ (L_n), ($n = 8, 12, 14, 16, 18, 20$). Amphiphilic polypeptides were dissolved in ethanol and the solutions were injected into water and heated at $90\text{ }^\circ\text{C}$ for 10 min.

3.2 Helicity of Hydrophobic Chain

The shape of the assembly depends on both the length and the helicity of the hydrophobic block. Here, an amphiphilic polypeptide incorporated with *D*-leucine, $(\text{Sar})_{25}\text{-}b\text{-(D-Leu-Aib)}_6$ (dL12), was synthesized and formed a left-handed helix (Figure 3). As expected, dL12 also formed a nanotube assembly. However, an equimolar mixture of enantiomeric peptides, L12 and dL12, demonstrated another shape, a vesicle of 180 nm diameter after heating at $90\text{ }^\circ\text{C}$ (Figure 5). The enantiomeric helix is known to form a stereo complex that is thermodynamically more stable than a single component. The isotropic packing induces the spherical structure; although, the single amphiphilic components form tube structures.

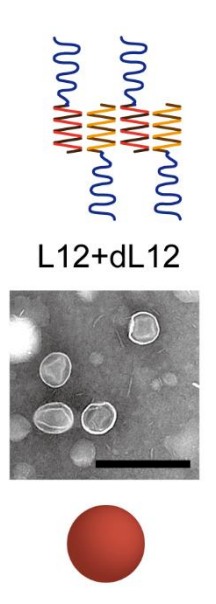


Figure 5. Schematic illustration and TEM images of peptide assemblies prepared from an enantiomeric mixture of L12 and dL12. The mixture was dissolved in ethanol and the solutions were injected into water and heated at 90 °C for 60 min. The assemblies were negatively stained by 2% samarium acetate for TEM observation. Scale bar: 500 nm.

4 Integration of Assembled Polypeptides

4.1 Mismatch of Hydrophobic Block

Assembly can be integrated by two kinds of peptide membrane. As shown above, the packing of an amphiphile, especially the hydrophobic block, defines the morphology of the assembly. An enantiomeric peptide tends to form a stereo complex, but peptides with the same helicity do not mix to form one membrane. Two kinds of amphiphilic polypeptides, which having the same helicity but the different lengths of the hydrophobic block, are divided into two membranes of the same length of the hydrophobic helix. In other words, these amphiphiles phase separate in one assembly.

Actually, a mismatch in the length of the hydrophobic block induces phase separation. L16 is composed of polysarcosine 32mers and a hydrophobic leucine-based 16 residue block. As shown above, L16 self-assembles into spheres with approximately 70–100 nm diameters in buffer after heating the planar sheets. This diameter is similar to the diameter of L12 nanotubes. Therefore, L16 and L12 were mixed to obtain an AB-type conjugate morphology. L16 planar sheets were incubated with L12 nanotubes at a ratio of 1:1 (w/w), and the dispersion was heated at 90 °C for 1 h.

As shown in Figure 6a, a nano-test-tube-shaped self-assembly with round bottoms were predominantly observed. The sizes of the neck and round-bottom parts of the assemblies correspond to those of the L12 nanotube and L16 sphere, respectively. Furthermore, the membrane thickness of the spherical part was 6 nm, which was the same as that of the L16 sphere. These results suggest that the nano-test-tube-shaped self-assembly was composed of a peptide membrane where L12 and L16 phases separated to form the corresponding neck part and spherical part of the nano-test-tube morphology.

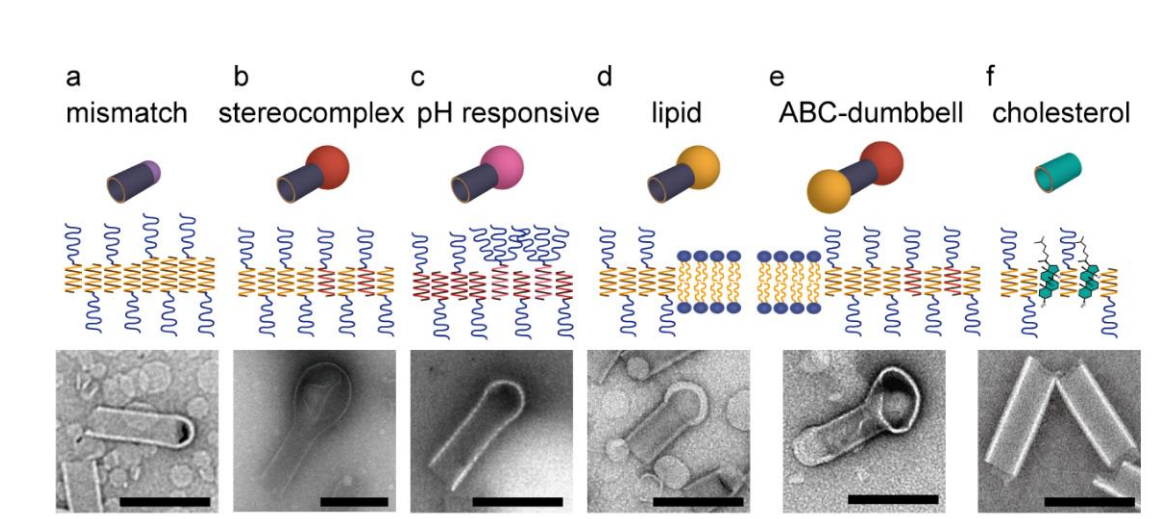


Figure 6. Schematic illustration and TEM images of assembly integrations. Assembly integrations were prepared from a combination of some amphiphilic polypeptides: (a) (Sar)₂₅-b-(L-Leu-Aib)₆ (L12) and (Sar)₃₂-b-(L-Leu-Aib)₈ (L16), (b) L12 and dL12, (c) ((Sar)₂₆)₃-b-((L-

His)₂-(L-Leu-Aib)₆) (HL12) and (Sar)₂₅-*b*-(D-Leu-Aib)₆ (dL12), (d) L12 and phospholipid (DPPC), (e) L12, dL12 and DPPC, and (f) L12 and cholesterol. Each mixture was dissolved in ethanol and the solutions were injected into water and heated at 90 °C for 60 min. The assemblies were negatively stained by 2% samarium acetate for TEM observation. Scale bar: 200 nm.

4.2 Combination with Stereo Complex Assembly

A combination of a stereo complex membrane prepared from L12 and dL12, and a single component membrane of L12 also formed successfully an integrated assembly that formed a round-bottom flask shape (Figure 6b). As mentioned above, the stereo complex membrane of L12 and dL12 formed a sphere shape of 180 nm diameter. Thus, when the stereo complex membrane was incubated with the L12 nanotube in saline and the mixture heated at 90 °C for 1 h, the stereo complex membrane attached to the open mouth of the L12 nanotube through hydrophobic interactions and then rolled-up to form a vesicle that capped the open mouth. The size of spherical part is corresponding to that of stereo complex vesicle from L12 and dL12.

4.3 Combination with pH-Dependent Assembly

Here, we introduce a stimuli-responsive molecule selectively into one of the parts of the self-assemblies. A pH-responsive polypeptide termed HL12, (poly(sarcosine)₂₆)₃-*b*-((L-His)₂-(L-Leu-Aib)₆), was prepared⁴³. Since HL12 contains a histidine (His) dipeptide at the junction between the hydrophilic block and the hydrophobic helical block, it was found that disassembly of either the neck or the round-bottom parts of the Janus-type assemblies under acidic conditions with heat treatment would facilitate self-assembly of HL12 into either part. The integration of HL12 enabled preparation of the round-bottom flask-shaped assemblies containing HL12 selectively either in the neck part⁴³ or the round-bottom part (Figure 6c).

The formation of a stereo complex between the right- and the left-handed helices was the basis for creating round-bottom flask-shaped assemblies with dL12 and HL12. The concavo-convex interaction between neighboring α -helical blocks defined precisely the size and shape of the molecular assemblies. Further, the amphiphilic helical peptides were allowed to diffuse laterally in the assemblies at high temperatures⁴³.

The pH-sensitive molecule, HL12, can be confined selectively into one part of the Janus-type assembly of the round-bottom flask-shaped assembly with a suitable combination of other amphiphilic helical peptides. The part containing HL12 can be selectively disrupted by acidification and heat treatment while leaving the other part of the Janus-type assembly intact. By using a combination of some functional amphiphiles, integration of not only structures but also functions also be succeeded.

4.5 Combination with Lipid Assembly

A lipid assembled liposome also be integrated into a nanostructure assembly. The sealing of a nanotube formed by amphiphilic polypeptides was performed using a liposome. The liposome was generated by mixing dipalmitoyl-phosphatidylcholine (DPPC) and cholesterol at a molar ratio of 55/45. The mixture in ethanol was injected into the L12 nanotube suspension (molar ratio of DPPC/L12, 1/1) in buffer and heated at 90 °C for 1 h. As a result, a round-bottom flask assembly was observed (Figure 6d). The sizes of the diameter and length of the neck part of the round-bottom flask were similar to those of the L12 nanotube. The membrane thickness of the neck part was ca. ~10 nm, which was the same as that of the L12 nanotube, indicating clearly that the neck part was composed of L12. On the other hand, the round bottom part of the round-bottom flask showed a smaller morphology than the liposome, and a membrane thickness of ca. 15 nm, which is obviously larger than that of the liposome, suggesting that the round-bottom shaped membrane is composed of a mixture of DPPC, cholesterol and L12.

4.6 ABC-Type Phase-Separated Assemblies

As shown some combinations, any amphiphiles form a unique assembly on the edge of L12 nanotube, resulting that complex morphologies are obtained by the assembly integration. By using this assembly integration method, ABC-type dumbbell shaped assemblies were prepared and observed. Two different vesicles and one nanotube were prepared from three types of amphiphilic helical peptides by phase separation. First, round-bottom flask assemblies were prepared from a mixture of L12 and dL12 at a molar ratio of 2:8 and purified using a syringe filter to remove assemblies larger than 450 nm. Subsequently, a DPPC solution was added and the mixture was heated at 90 °C for 1 h. By using this two-step method, ABC-type asymmetric dumbbell-shaped assemblies were obtained. As shown in Figure 6e, the asymmetric dumbbell-shaped morphology had two different spherical parts that were each composed of 180-nm stereoscope vesicles of L12 and dL12 and size-uncontrolled DPPC liposomes, and a middle neck part that was the L12 nanotube with a diameter of 80 nm and a length of 180 nm.

4.7 Conjugate with Cholesterol

In addition to these shape controls, membrane fluidity of the polypeptide assemblies can be controlled by conjugation with cholesterol. Polypeptide nanotube rigidity was increased and displayed higher stability following insertion of cholesterol into the peptide membrane without changing the shape of the assembly. When the membrane fluidity was evaluated by Laurdan reagent, the fluidity increased linearly as the amount of incorporated cholesterol increased. Controlling fluidity is important for further applications of polypeptide assemblies.

5 Conclusions

Using amphiphilic polypeptides, it is possible to prepare different nanostructure shapes, such as fibers, sheets, spheres and tubes. In addition, by summation of these nanostructures more complex shapes were prepared. These complex structures are expected to contribute to the fine regulation of various nanosystems. Nanosystem also become to need on demand precise

shape- and size-control to improve the function in near future. Development of bottom-up method to prepare various complex morphology is very important challenge. This work in this chapter is one of their advanced methods, show the possibility of molecular assembly integration and give knowledge to establish complex-shaped nanomaterials for researchers in various fields.

References

1. Lehn, M. J. *Science*, **1993**, 260, 1762–1763.
2. Whitesides, M. G. *Science*, **2002**, 295, 2418–2421.
3. Aida, T.; Meijer, W. E.; Stupp, I. S. *Science*, **2012**, 335, 813–817.
4. Philp, D.; Stoddart, F. J. *Angew. Chem. Int. Ed.*, **1996**, 35, 1154–1196.
5. Arnon, A. Z.; Vitalis, A.; Levin, A.; Michaels, T. C. T.; Caflisch, A.; Knowles, J. P. T.; Adler-Abramovich, L.; Gazit, E. *Nat. Commun.*, **2016**, 7, 13190.
6. Tao, K.; Makam, P.; Aizen, R.; Gazit, E. *Science*, **2017**, 358, eaam9756.
7. Zhang, S. *Nat. Biotechnol.*, **2003**, 21, 1171–1178.
8. Webber, J. M.; Appel, A. E.; Meijer, W. E.; Langer, R. *Nat. Mater.*, **2015**, 15, 13–26.
9. Reches, M.; Gazit, E. *Science*, **2003**, 300, 625–627.
10. Adler-Abramovich, L.; Aronov, D.; Beker, P.; Yevnin, M.; Stempler, S.; Buzhansky, L.; Rosenman, G.; Gazit, E. *Nat. Nanotechnol.*, **2009**, 4, 849–854.
11. Reches, M.; Gazit, E. *Nat. Nanotechnol.*, **2006**, 1, 195–200.
12. Berger, O.; Adler-Abramovich, L.; Levy-Sakin, M.; Grunwald, A.; Liebes-Peer, Y.; Bachar, M.; Buzhansky, L.; Mossou, E.; Forsyth, T. V.; Schwartz, T.; Ebenstein, Y.; Frolow, F.; Shimon, W. J. L.; Patolsky, F.; Gazit, E. *Nat. Nanotechnol.*, **2015**, 10, 353–360.
13. Gazit, E. *Chem. Soc. Rev.*, **2007**, 36, 1263.

General Introduction

14. Frederix, M. J. W. P.; Scott, G. G.; Abul-Haija, M. Y.; Kalafatovic, D.; Pappas, G. C.; Javid, N.; Hunt, T. N.; Ulijn, V. R.; Tuttle, T. *Nat. Chem.*, **2014**, 7, 30–37.
15. Adler-Abramovich, L.; Gazit, E. *Chem. Soc. Rev.*, **2014**, 43, 6881–6893.
16. Yan, X.; Zhu, P.; Li, J. *Chem. Soc. Rev.*, **2010**, 39, 1877.
17. Fleming, S.; Ulijn, V. R. *Chem. Soc. Rev.*, **2014**, 43, 8150–8177.
18. Yakimov A., Rychkov G., Petukhov M. *Methods Mol. Biol.* **2014**;1216:1–14.
19. Estieu-Gionnet K., Guichard G. *Expert Opin. Drug Discov.* **2011**, 6 (9), 937–963.
20. Robertson N. S., Jamieson A. G., *Repts Organic Chem.* **2015**, 5, 65–74.
21. Finkelstein A. V., Badretdinov A. Y., Ptitsyn O. B. *Proteins* **1991**, 10(4), 287–299.
22. Doig A. J. *Biophys. Chem.* **2002**, 101-102, 281–293.
23. Petukhov M., Tatsu Y., Tamaki K., Murase S., Uekawa H., Yoshikawa S., Serrano L., Yumoto N. *J. Pept. Sci.* **2009**, 15 (5), 359–365.
24. Villegas V., Viguera A. R., Aviles F. X., Serrano L. *Fold Des.* **1996**, 1 (1), 29–34.
25. Surzhik M. A., Churkina S. V., Shmidt A. E., Shvetsov A. V., Kozhina T. N., Firsov D. L., Firsov L. M., Petukhov M. G., *Applied biochemistry and microbiology.* **2010**, 46 (2), 206–211.
26. Scholtz J. M., Baldwin R. L. *Annu. Rev. Biophys. Biomol. Struct.* **1992**, 21, 95–118.
27. Munoz V., Serrano L. *Nat. Struct. Biol.* **1994**, 1 (6), 399–409.
28. Creamer T. P., Rose G. D. *Proteins.* **1994**, 19 (2), 85–97.
29. Doig A. J., Baldwin R. L. *Protein Sci.* **1995**, 4 (7), 1325–1336.
30. Stapley B. J., Rohl C. A., Doig A. J. *Protein Sci.* **1995**, 4 (11), 2383–2391.
31. Munoz V., Serrano L. *J. Mol. Biol.* **1995**, 245 (3), 275–296.
32. Petukhov M., Munoz V., Yumoto N., Yoshikawa S., Serrano L. *J. Mol. Biol.* **1998**, 278 (1), 279–289.

33. Petukhov M., Uegaki K., Yumoto N., Yoshikawa S., Serrano L. *Protein Sci.* **1999**, 8 (10), 2144–2150.
34. Petukhov M., Uegaki K., Yumoto N., Serrano L. *Protein Sci.* **2002**, 11 (4), 766–777.
35. Popot, L. J.; Engelman, M. D. *Annu. Rev. Biochem.*, **2000**, 69, 881.
36. Dixon, M. A.; Stanley, J. B.; Matthews, E. E.; Dawson, P. J.; Engelman, M. D. *Biochemistry*, **2006**, 45, 5228.
37. Heijne, V. G. *EMBO J.*, **1986**, 5, 3021.
38. Mackenzie, R. K. *Chem. Rev.*, **2006**, 106, 1931.
39. Oehlke, J.; Scheller, A.; Wiesner, B.; Krause, E.; Beyermann, M.; Klauschenz, E.; Melzig, M.; Bienert, M. *Biochim. Biophys. Acta*, **1998**, 1414, 127.
40. Tossi, A.; Sandri, L.; Giangaspero, A. *Biopolymers*, **2000**, 55, 4.
41. Wagstaff, M. K.; Jans, A. D. *Curr. Med. Chem.*, **2006**, 13, 1371.
42. Huey W. Huang. *J. Phys. II France* 5, **1995**, 1427–1431.
43. Ueda, M.; Uesaka, A.; Kimura, S. *Chem. Commun.* **2015**, 51, 1601–1604.
44. Ueda, M.; Makino, A.; Imai, T.; Sugiyama, J.; Kimura, S. *Polym. J.* **2013**, 45, 509–515.
45. Ueda, M.; Makino, A.; Imai, T.; Sugiyama, J.; Kimura, S. *Soft Matter* **2011**, 7, 4143–4146.
46. Ueda, M.; Makino, A.; Imai, T.; Sugiyama, J.; Kimura, S. *Langmuir* **2011**, 27, 4300–4304.
47. Ueda, M.; Makino, A.; Imai, T.; Sugiyama, J.; Kimura, S. *Chem. Commun.* **2011**, 47, 3204–3206.
48. Ueda, M.; Makino, A.; Imai, T.; Sugiyama, J.; Kimura, S. *J. Pept. Sci.* **2011**, 17, 94–99.
49. Griffin, W. C. *Journal of the Society of Cosmetic Chemists* **1949**, 1, 311–326.
50. Griffin, W. C. *Journal of the Society of Cosmetic Chemists* **1954**, 259.

General Introduction

51. Devies, J. T. A Quantitative Kinetic Theory of Emulsion Type. I Physical Chemistry of the Emulsifying Agent. In Gas/Liquid and Liquid/Liquid Interfaces.; Proceedings of 2nd International Congress Surface Activity; Butterworths, London, **1957**.
52. Israelachvili, J. N. Intermolecular and Surface Forces, Third Edition; 3rd ed.; Academic Press, **2010**
53. Kanzaki, T.; Horikawa, Y.; Makino, A.; Sugiyama, J.; Kimura, S. *Mcromol. Biosci.* **2008**, 8, 1026–1033.

Chapter 2

Spontaneous Formation of Gating Lipid-Domain in Uniform-Size Peptide Vesicles for Controlled Release

Introduction

In chemotherapy, an optimal rate and release mechanism of the drug from the carrier are important issues for the therapeutic performance of the drug at the target site. The lipidic membrane of liposomes has a natural sol-gel phase transition and these lipid systems are a promising tool for temperature-responsive release of drugs.¹ However, the clinical use of liposomes is limited because of their low physical stability caused by the high shear rate of blood circulation around tiny vessels²⁻⁴ or by the high osmotic pressure that occurs upon injection of these lipid species.⁵ Thus, higher mechanical stability of a drug delivery system (DDS) carrier is required for the controlled release at the target tissue when delivering the drug through the bloodstream.

In recent years, polymer-lipid hybrid assemblies⁶⁻⁹ have attracted the attention of researchers as versatile materials for used in various fields, including drug delivery,¹⁰ molecular recognition on liposomes¹¹⁻¹² and membrane models.¹³⁻¹⁴ Mixing an amphiphilic polymer with a lipid leads to the formation of a homogeneous or heterogeneous phase-separated membrane.¹⁵⁻¹⁷ A heterogeneous membrane allows the hybrid assembly to display dual membrane functions simultaneously. However, most current hybrid vesicle forming heterogeneous membranes have a polymer or a peptide domain as a raft in a sea of membrane lipids with the polymeric domain acting as an artificial biomimetic functional block such as a channel protein.¹⁸ In addition, in most previous reports, a micro-ordered hybrid vesicle has been used because these vesicles are easier to observe under a microscope, thereby facilitating fundamental research such as a phase diagram and membrane modeling.

Here, to achieve both nano-structured high stability and the thermosensitive release of drugs, we attempted to prepare a potential gating lipid domain in a stable polypeptidic vesicle. We found a peptide-lipid hybrid vesicle (PLHV) composed of 1,2-dimyristoyl-sn-glycero-3-phosphocholine (DMPC) within a sea of amphiphilic block co-polypeptide composed of poly(sarcosine) and poly(L-leucine-2-aminoisobutyric acid), (poly(Sar)₂₆-(L-Leu-Aib)₇,

S26L14) (Figure 1). The hydrophobic alternating Leu-Aib copolymer of S26L14 folds to form an α -helix structure that induces tight bundle packing between helices to facilitate formation of a polypeptide membrane,¹⁹⁻²³ the spontaneous formation of a phase-separated membrane structure with a lipid was expected. As a result, the polypeptide domain controlled the uniform hybrid assembly and gating lipid domain, which allowed the temperature-responsive release of fluorescein isothiocyanate-labeled polyethylene glycol (FITC-PEG) due to its phase-transition phenomena. The morphology and stability of the hybrid vesicle were investigated over one month. In addition, the phase-transition temperature shift and uniform size of the hybrid vesicle are discussed.

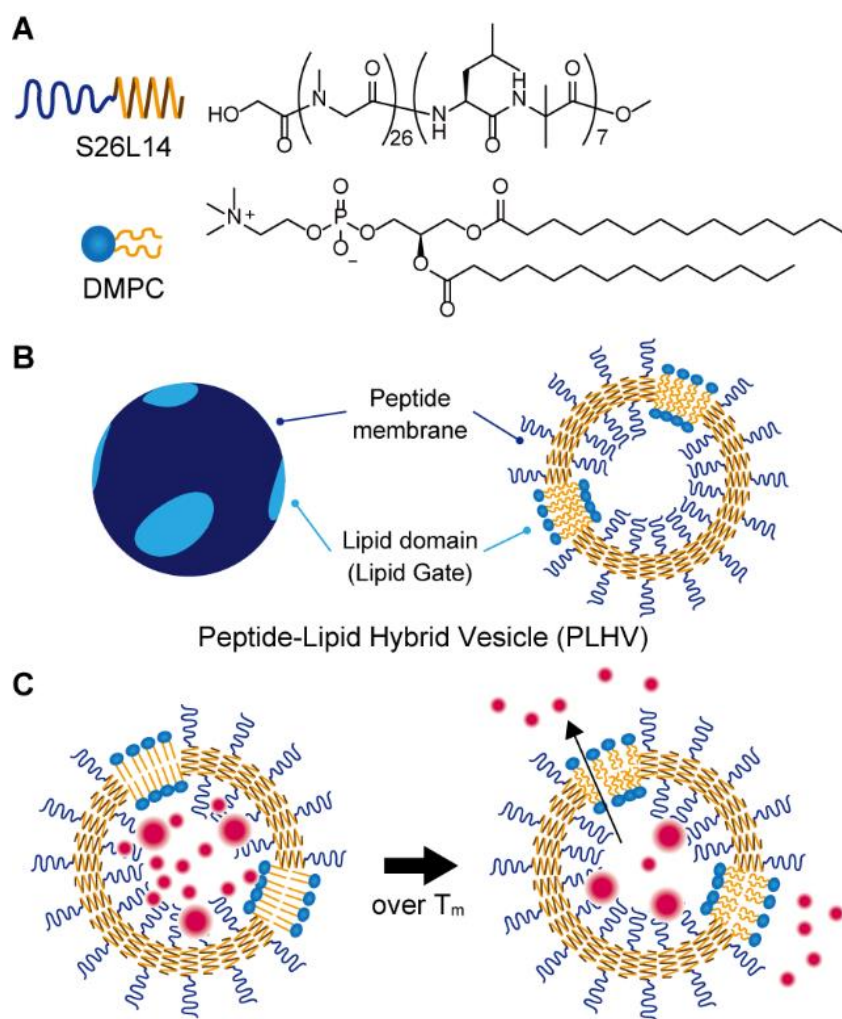


Figure 1. Chemical structure of the amphiphilic polypeptide S26L14 and phospholipid DMPC (A) and schematic illustrations of the peptide-lipid hybrid vesicle (PLHV) (B) and its temperature-responsive release through the lipid domain (C).

Experimental Section

Preparation of Molecular Assemblies. Peptide-lipid hybrid vesicles, peptide assemblies and liposomes were prepared by the ethanol injection method. Amphiphilic polypeptide (20 mg) and lipid (20 mg) were dissolved in ethanol (400 μ L) as stock solutions. Different formulations

were then prepared by the ethanol injection method while keeping the molar ratio at 1:1 (S26L14:DMPC). Briefly, an aliquot (a mixture of peptide and DMPC or peptide only (10 μ L), or DMPC only (10 μ L)) of the peptide-lipid ethanol solution, peptide solution, or lipid solution was injected into saline (150 mM NaCl, pH 7.4, 1 mL) with stirring at 25 °C and then the dispersions were heated at 90 °C for 1 h.

Preparation of Molecular Assembly from Peptide S26L14 and Different Lipids, DMPC, DPPC and DSPC. Hybrid vesicles were prepared using different lipids and S26L14. Stock solutions and preparation methods were the same as described above. Different formulations were then prepared keeping the molar ratio at 1:1 and 4:1 for each sample: S26L14+DMPC, S26L14+DPPC and S26L14+DSPC.

Molecular Assemblies Prepared from Peptide, S26L14 and Different Molar Ratios of DMPC. The peptide-lipid molar ratios (ranging from 0.25 to 100) were 0.25, 1, 2, 4, 10 and 20. These assemblies were prepared using the above-mentioned methods.

Transmission Electron Microscopy (TEM). TEM images were taken using a JEOL JEM-1230 at an accelerating voltage of 80 kV. For observations, a drop of dispersion was mounted on a carbon-coated Cu grid (Okenshoji Co., Ltd., Japan) and stained negatively with 2% samarium acetate, followed by removal of the excess fluid with a filter paper.

Dynamic Light Scattering (DLS). The hydrodynamic diameter of molecular assemblies in saline was analyzed by ELSZ-2PL (Photal Otsuka Electronics, Japan) using a He-Ne laser. Measurements were performed at 25 °C.

Fluorescent Spectroscopy. The fluorescent spectra of assembled dispersions were obtained using a JASCO FP-6500 spectrofluorometer at 25 °C with a transmission cell.

Förster Resonance Energy Transfer (FRET) Analysis. FRET experiments in vesicles were carried out using a fluorometer (Microplate Flash Reader, PerkinElmer, Waltham, MA, USA).

For the NBD-PE/Rhodamine-PE donor/acceptor pair, the excitation wavelength was set at 460 nm and emission spectra were collected from 480 to 650 nm. FRET was measured in liposomes containing known concentrations of donor- and acceptor-labeled vesicles.

Hybrid vesicles were labeled with 0.8 mol % of both NBD-PE and Rhod-PE. Briefly, for hybrid vesicles composed of polypeptides and DMPC, stock ethanol solutions of S26L14, DMPC, NBD-PE and Rhod-PE were mixed to give the desired ratio (S26L14, DMPC, NBD-PE, Rhod-PE; 73, 73, 0.58, 0.58 nmol) and then injected into saline (1 mL) simultaneously. The mixture was then stirred and heated in the same manner described before (hybrid vesicle assembly section). Similarly, two kinds of DMPC liposome samples containing NBD-PE and Rhod-PE were prepared for FRET analysis as control samples with particular mixing ratios (DMPC, NBD-PE, Rhod-PE; 73, 0.58, 0.58 and 146, 0.58, 0.58 nmol). In addition, respective donor-labeled (NBD-PE only) vesicles were also prepared to calculate the FRET efficiency E in the absence and presence of the acceptor according to $E (\%) = (I_D - I_{DA}) / (I_D) \times 100$, where I_D and I_{DA} are the donor intensities of samples containing only donor-labeled vesicles and samples with both donor- and acceptor-labeled vesicles, respectively.

Circular Dichroism (CD). CD measurements were carried out on a JASCO J-720 (JEOL, Japan) using a cell with an optical path length of 1 cm. Data was recorded at 25 °C. 0.35 mM peptide was used for self-assembly in saline, and the dispersion was diluted five-fold before CD data collection.

Laurdan Test. The membrane fluidity of PLHVs, S26L14 nanotubes and DMPC liposomes were measured with *N,N*-dimethyl-6-dodecanoyl-2-naphthylamine (Laurdan). Laurdan is a fluorescent dye that is sensitive to the polarity of its surrounding environment. A general polarization value, GP_{340} , was calculated: $GP_{340} = (I_{440} - I_{490}) / (I_{440} + I_{490})$, where I_{440} and I_{490} are emission intensities at 440 and 490 nm of excited Laurdan at 340 nm. The temperature range of 10–42 °C was controlled by a circulating water bath.

Differential Scanning Calorimetry (DSC). DSC is used widely to detect the phase transition of liposomes and other molecules. Desired concentrations of 20 μL of self-assembled hybrid vesicles, DMPC liposomes, or peptide nanotubes were placed on aluminum pans that were sealed with lids. A reference sample pan with saline only was also used. The temperature range for scanning samples was 10–60 $^{\circ}\text{C}$ with a heating rate of 1 $^{\circ}\text{C}/\text{min}$.

FITC-PEG Loading and Release Study. Three millimolar of FITC-PEG was used to examine the self-quenching property. Desired molar ratios of hybrid vesicles and DMPC liposome stock solutions were injected into saline containing FITC-PEG and stirring for 2 h, and then heated at 90 $^{\circ}\text{C}$ for 1 h. The samples were then passed through a Millipore centrifuge filter unit (30 kDa molecular weight cutoff) using a centrifugation speed of 2000 rpm at 4 $^{\circ}\text{C}$ to remove free FITC-PEG. The loading efficiency of FITC-PEG was calculated as: $(F_{\text{af}} / F_{\text{bf}}) \times 100$. F_{af} = fluorescence intensity after the centrifuge filter pass and F_{bf} = fluorescence intensity before the centrifuge filter pass. The fluorescence dequenching assay was used to determine the FITC-PEG release from hybrid vesicles and DMPC liposomes. In brief, 100 μL of FITC-PEG-loaded hybrid vesicles or DMPC liposomes were injected into 10 mL of saline and mixed homogeneously. At 0.5, 1, 2 and 4 h intervals, 1 mL of the samples were taken and cooled on ice to stop further drug release. The release rate of FITC-PEG was calculated using the following equation: $\text{Release rate (\%)} = (F - F_0) / (F_{100} - F_0) \times 100$, where F is the fluorescence intensity of the sample at a specific point, F_0 is the background fluorescence of the sample and F_{100} is the maximum fluorescence release from the lysed carrier by lysis buffer, which was the average of three samples. We added lysis buffer (Code# CK12, Lot. KU749, Dojindo Molecular Technologies, INC., Japan) (5 μL) into FITC-PEG loaded hybrid vesicle dispersions (1 mL) and heated dispersions to 60 $^{\circ}\text{C}$ for 10 min to obtain the F_{100} value. A JASCO FP-6500 fluorescence spectrometer was used with excitation and emission wavelengths of 490 and 520 nm, respectively. The temperatures used for this release study were 4, 37 and 42 $^{\circ}\text{C}$. The molecular weight of PEG was 2 and 5 kDa.

Results and Discussion

Morphology of the Peptide-Lipid Hybrid Vesicle (PLHV).

The morphology of assemblies prepared from a combination of amphiphilic polypeptide S26L14 and lipid (DMPC, 1,2-dipalmitoyl-sn-glycero-3-phosphocholine (DPPC), or 1,2-distearoyl-sn-glycero-3-phosphocholine (DSPC)) at molar ratios of 1:1 was observed by transmission electron microscopy (TEM) (Figure 2D and 3). A vesicular assembly with a uniform diameter of 75 nm was obtained when a mixture of S26L14 and DMPC was injected into saline and the dispersion was heated at 90 °C for 1 h. S26L14 formed a nanotube with a uniform diameter and length of 80 nm and 200 nm, respectively (Figure 2I), as reported previously.^{20, 24} In contrast, DMPC formed various sized liposomes using the same preparation method with diameters of 10–10,000 nm (Figure 2A). The assembly shape of the PLHV was clearly different from those of the pure components. Dynamic light scattering (DLS) analysis also showed different sizes among assemblies (Figure 2J and Table 1); PLHV, S26L14 nanotubes and DMPC liposomes were 76 nm, 145 nm and 2286 nm in diameter, respectively. These results indicate that S26L14 and DMPC co-assembled to form a hybrid vesicle. The “uniform” size of the PLHVs probably arises from S26L14 forming a curved sheet domain with a uniform curvature (Figure 4) within a hybrid membrane.

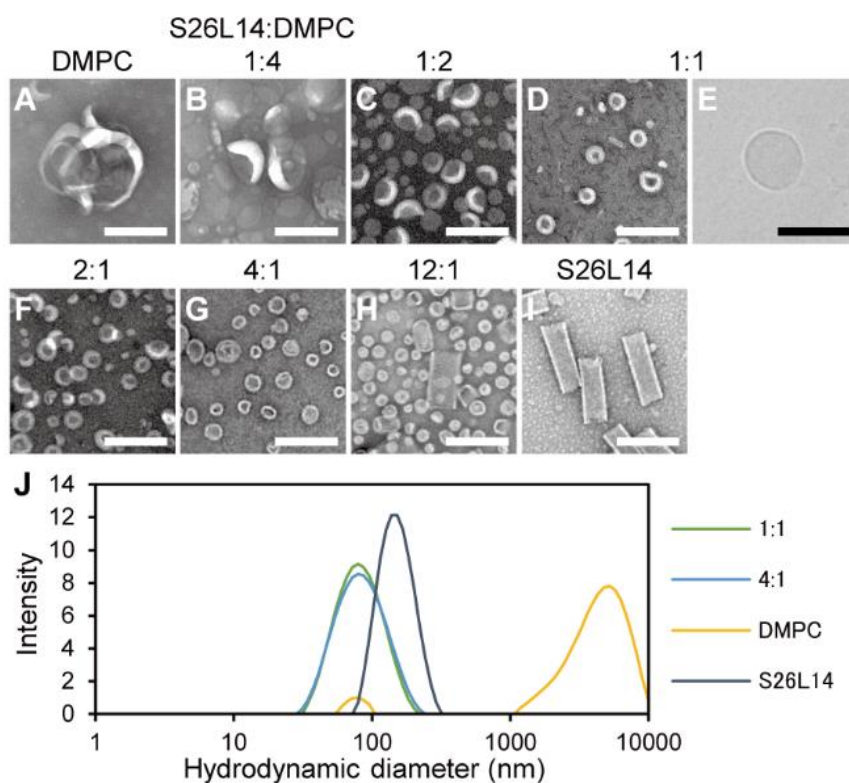


Figure 2. TEM images of assemblies prepared from combining the amphiphilic polypeptide S26L14 and DMPC at various mixing ratios: (A) 0:1, (B) 1:4, (C) 1:2, (D) 1:1, (F) 2:1, (G) 4:1, (H) 12:1 and (I) 1:0. A cryo-TEM image of the assembly from an equimolar mixture of S26L14 and DMPC (E). Size distribution of each assembly with a mixing ratio of 1:1 (green line) and 4:1 (blue line), DMPC liposomes (yellow), and the S26L14 nanotubes (black) (J). Scale bar is 200 nm.

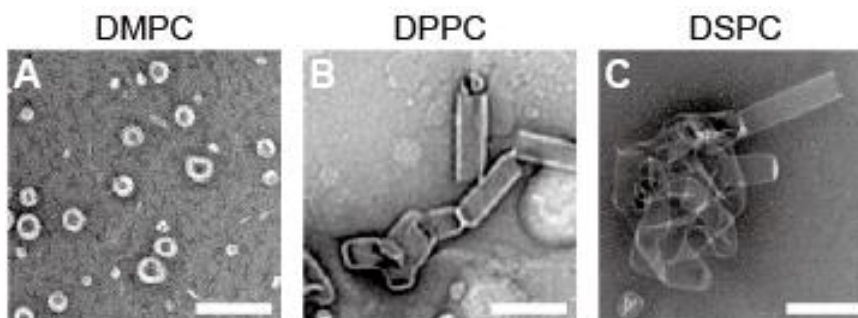


Figure 3. TEM images of hybrid assemblies prepared from a mixture of S26L14 and DMPC (A), DPPC (B) or DSPC (C) with a mixing molar ratio of 1:1.

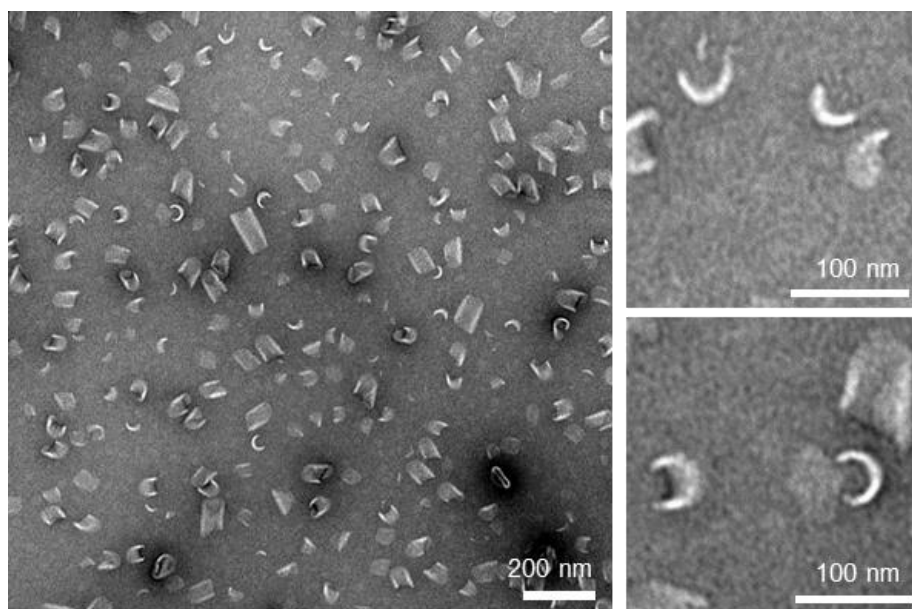


Figure 4. TEM images of S26L14 nanosheets prepared by the ethanol injection method without heat treatment.

Combining S26L14 with DPPC and DSPC yielded aggregates containing tubular and roundish structures, respectively (Figure 3). These lipids appear to act as a roundish joint between the S26L14 nanotubes and phase-separate due to the weak miscibility of S26L14, which probably occurs because of a large mismatch of the lengths between the hydrophobic blocks and the lipid moieties.

We next investigated the effect of the mixing ratio of PLHVs. In S26L14/DMPC ratios of 1:4 and 1:2, a liposome-like hybrid assembly was observed. The sizes of the assemblies were not uniform and ranged from 50 to 2000 nm (Figure 2B and 2C). The membrane thickness of PLHV was similar to that of DMPC liposomes (Figure 2A). Molar ratios of 1:1, 2:1 and 4:1,

yielded PLHVs with uniform diameters of 75 nm (Figure 2C–G). From dynamic light scattering (DLS) measurement, these PLHVs showed a polydispersity index of approximately 0.1 (Table 1). In contrast, a 12:1 mixture showed not only 75 nm-sized hybrid vesicles but also nanotubes in the dispersion (Figure 2H). These morphological results are explained by the ratio of calculated occupied surface areas as follows. The occupied surface area of an α -helix block of S26L14 and DMPC is regarded as 1.50²⁵ and 0.66 nm².²⁶⁻²⁷ For the molar ratio of 1:4, the surface area ratio of S26L14:DMPC was 36:64. The contribution from the lipid membrane dominates at this mixing ratio and a liposome-like assembly was observed. For 1:1, 2:1 and 4:1 ratios, the surface area ratios of S26L14:DMPC were 69:31, 82:18 and 90:10, respectively (Table 1). For these ratios, the morphology of the PLHV is dominated by the contribution from S26L14. The composition ratio of S26L14 and DMPC in PLHV1-1 was evaluated after dialysis, which removes free S26L14 and DMPC. The content of S26L14 was estimated by its absorbance at 220 nm and that of DMPC was determined by using a phospholipid quantitative determination kit, respectively. According to the results, PLHV1-1 was composed of S26L14 and DMPC at a molar ratio of 1:0.83, which is close to the initial mixing ratio of 1:1 (Table 2).

Table 1. DLS Results of Each Assembly and Theoretical Occupied Area of S26L14 and DMPC for Each Assembly.

	Ratio (%)	D_H (nm)	PDI	Theoretical occupied area ratio (%)	Shape
DMPC	0:100	2286	0.87	0:100	Various sized vesicle
PLHV1-4	20:80			36:64	Various sized vesicle
PLHV1-2	33:67			53:47	Various sized vesicle
PLHV1-1	50:50	75.5	0.11	69:31	Uniform vesicle
PLHV2-1	67:33			82:18	Uniform vesicle
PLHV4-1	80:20	76.4	0.12	90:10	Uniform vesicle
PLHV12-1	92:8			96:4	Uniform Vesicle + Tube
S26L14	100:0	145.1	0.10	100:0	Tube

Table 2. Composition ratio of S26L14 and DMPC in PLHV.

	S26L14			DMPC			S26L14:DMPC
	Abs ₂₂₀	mg/mL	nmol/mL	Abs ₆₀₀	mg/mL	nmol/mL	
PLHV1-1	0.113	0.196	57.8	0.052	0.035	47.8	1:0.83

Peptide-lipid hybrid vesicles prepared from S26L14 and DMPC with ratios of 1:1 and 4:1 were named PLHV1-1 and PLHV4-1, respectively. These vesicles were stored at 4 °C for one month and their structural stability was evaluated by TEM observations and DLS analysis (Figure 5). The shape of the vesicles was maintained during this period. The polypeptide-rich hybrid vesicles showed high stability when compared with that of general liposomes. Thus, these hybrid vesicles have sufficient stability (i.e., at least one month) to be used as DDS carriers.

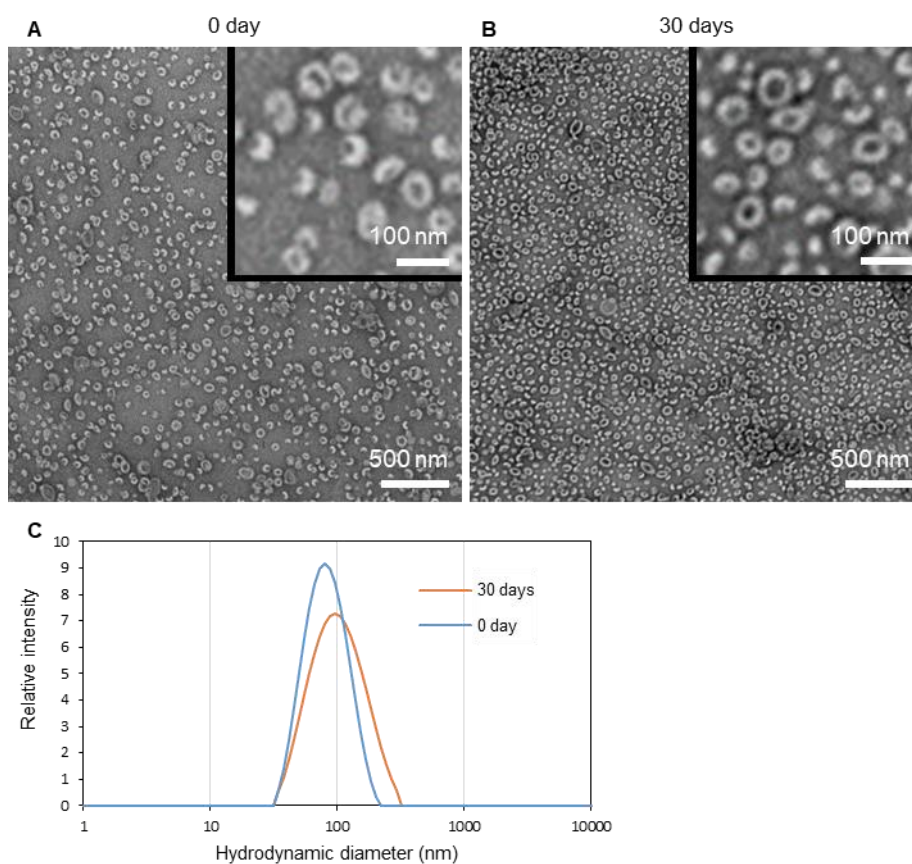


Figure 5. TEM images (A, B) and hydrodynamic diameter from DLS spectra (C) of PLHV1-1 before (A) and after 30 days (B) at 4 °C.

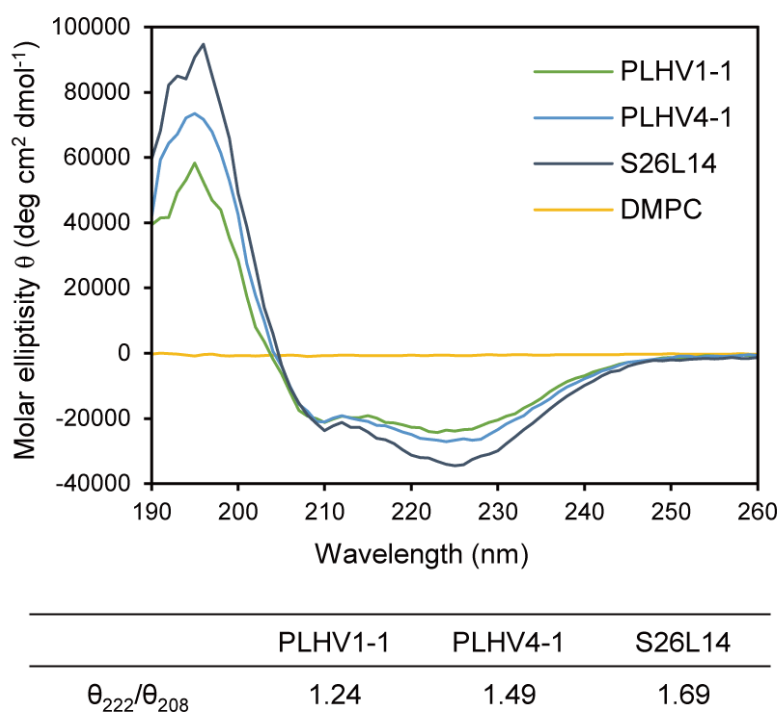


Figure 6. CD spectra of assembly dispersions prepared from pure S26L14 (black), S26L14 and DMPC with mixing ratios of 4:1 (blue) and 1:1 (green), and pure DMPC (yellow) and the intensity ratio of $\theta_{222}/\theta_{208}$ in saline.

Circular dichroism (CD) spectra of PLHV1-1, PLHV4-1, S26L14 nanotube and DMPC liposome dispersions supported the presence of a peptide domain in the hybrid vesicles. The data revealed that both peptide nanotubes and PLHVs displayed the characteristics of α -helical configurations, with double minima at 222 and 208 nm (Figure 6). The $\theta_{222}/\theta_{208}$ ratio of PLHV1-1, PLHV4-1 and S26L14 nanotubes were 1.24, 1.49 and 1.69, respectively. The strict packing

of S26L14 is evident because the ratio value >1 indicates a bundle formation of α -helices.²⁸⁻²⁹ The observed decrease of the $\theta_{222}/\theta_{208}$ ratio for the PLHVs is because DMPC inserted into the S26L14 membrane partially loosens the packing of the nanotube-forming S26L14. This results in PLHV1-1 and PLHV4-1 not forming nanotubes but spherical vesicles. Furthermore, CD spectra of PLHV1-1, PLHV4-1 and S26L14 assemblies at 26, 38 and 42 °C showed that temperature did not influence the secondary structure and bundle formation of the peptides (Figure 7).

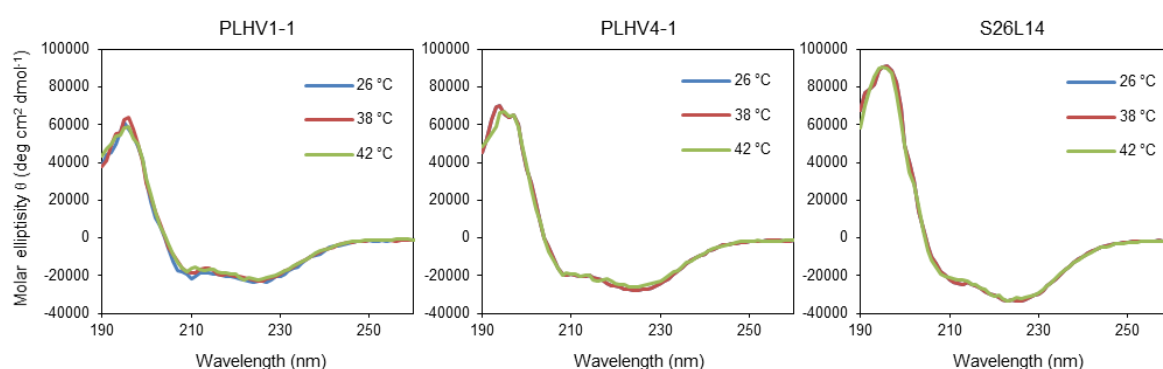


Figure 7. CD spectra of PLHV1-1, PLHV4-1 and S26L14 assembly dispersions at 38 and 42 °C.

Phase-Separation.

To investigate the homo/heterogeneity of PLHVs, fluorescence resonance energy transfer (FRET) analysis was performed using *N*-(7-nitro-2-1,3-benzoxadiazol-4-yl)-1,2-dipalmitoyl-sn-glycero-3-phosphoethanolamine (NBD-PE) and *N*-(lissamine rhodamine B sulfonyl)-1,2-dipalmitoyl-sn-glycero-3-phosphoethanolamine (Rhod-PE). NBD-PE and Rhod-PE act as the donor and acceptor for FRET measurements, respectively. For FRET analysis, a PLHV1-1 sample containing a mixture of S26L14 (73 nmol), DMPC (73 nmol), NBD-PE (0.6 nmol) w/o Rhod-PE (0.6 nmol) was prepared. As control samples, 73 nmol/mL and 146 nmol/mL DMPC liposomes, termed DMPC-73 and DMPC-146, containing NBD-PE (0.6 nmol) w/o Rhod-PE (0.6 nmol) were prepared.

Excitation of NBD-PE at 460 nm gave fluorescent spectra with a strong emission intensity of Rhod-PE in PLHV1-1 (Figure 8A) and the FRET efficiency was similar to that of the DMPC-73 dispersion (Figure 8B). Although the concentration of FRET dye pairs in PLHV1-1 and DMPC-146 are the same, the FRET efficiency was close to that of the higher dye/lipid ratio system DMPC-73 (Figure 8C). This demonstrated that PLHV1-1 had a heterogeneous phase-separated membrane and both DMPC and S26L14 domains existed, as shown in Figure 8C.

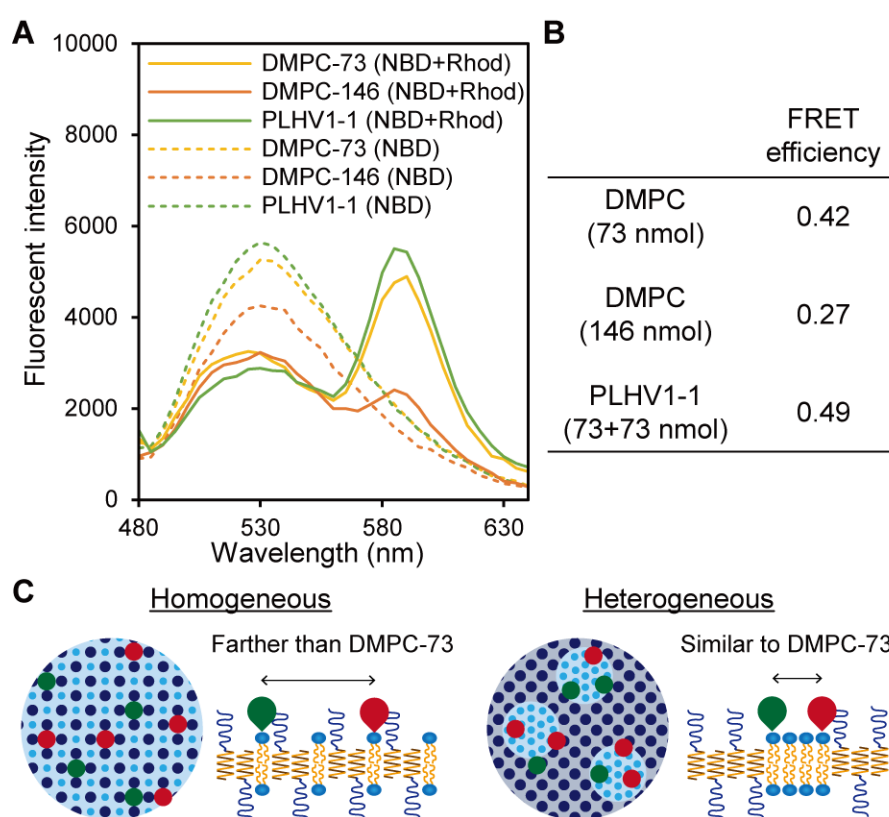


Figure 8. Fluorescent spectra and FRET efficiency of 73 and 146 nmol/mL DMPC liposomes and 73 + 73 nmol/mL PLHV1-1 containing NBD-PE (0.6 nmol) w/o Rhod-PE (0.6 nmol), which were measured by using excitation light at 460 nm (A and B). Schematic illustration of homogeneous and heterogeneous membranes in PLHVs and the distance between donor/accepter dyes.

Laurdan reagent (*N,N*-dimethyl-6-dodecanoyl-2-naphthylamine) can also be used as a molecular probe to monitor the heterogeneity of liposomes.³⁰⁻³² Laurdan shows specific emission peaks at 440 and 490 nm that originate from lipid membranes in liquid ordered (L_o) and liquid disordered phases (L_d), respectively.³¹⁻³² Figure 9 shows the fluorescence spectra of Laurdan in PLHV1-1, PHLV4-1, S26L14 nanotube and DMPC liposomes dispersions at 42 °C. A single peak at 490 nm was observed in the DMPC dispersion, whereas a single peak at 440 nm was observed in the S26L14 nanotube dispersion. These results indicated that DMPC liposomes and S26L14 nanotubes were in homogeneously disordered and ordered phases, respectively. In contrast, PLHV1-1 and PHLV4-1 exhibited emission peaks at both 440 and 490 nm, indicating the co-existence of disordered DMPC domains and ordered S26L14 domains in the hybrid vesicles.

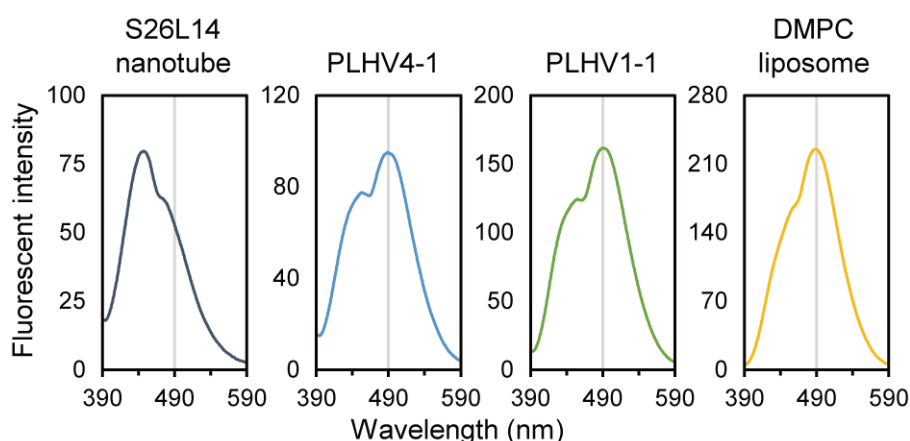


Figure 9. Fluorescent spectra of Laurdan in assemblies: S26L14 nanotube, PLHV1-1, PLHV4-1 and DMPC liposome dispersions.

Phase-Transition.

The generalized polarization, GP_{340} value, which was calculated from emission intensities of Laurdan at 440 and 490 nm by using excitation light at 340 nm, has been shown to be a useful indicator of the degree of hydration of the membrane surface.³³⁻³⁴ Investigating

the GP_{340} value as a function of temperature provided an approach to evaluate the phase-transition temperature. The GP_{340} value of S26L14 nanotubes from 10 to 42 °C was constant, indicating no phase-transition temperature (T_m) over this temperature range (Figure 10A). In contrast, the GP_{340} value for DMPC showed a drastic change at ~25 °C, which corresponds to the known T_m of DMPC. The GP_{340} value for PLHV1-1 and PLHV4-1 showed a decrease at ~35 °C. To confirm the phase-transition of the membrane, differential scanning calorimetry (DSC) measurements were also performed. The thermograms of PLHV1-1 and DMPC liposomes indicated that PLHV1-1 has a phase transition temperature of 38 °C, and DMPC liposomes have a value of ~23 °C (Figure 10B). Furthermore, the results from DSC analysis also showed that the S26L14 nanotube had no phase-transition temperature from 14 to 46 °C (Figure 10B). As mentioned above, CD spectra of PLHV at various temperatures (Figure 7) indicated that 42 °C did not affect the secondary structure of the peptide and bundle formation between peptides in PLHV. By taking these results into consideration, a phase-transition of a hybrid vesicle corresponding to a lipid domain and S26L14 did not influence the spectra.

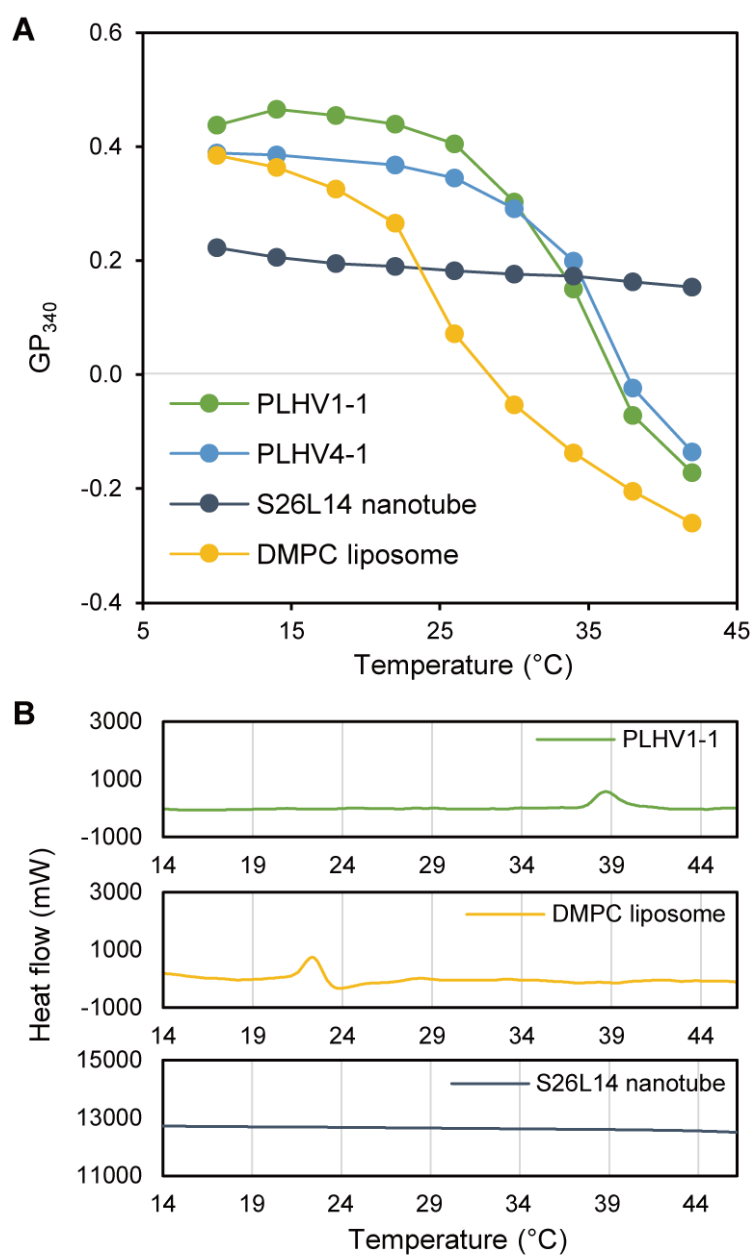


Figure 10. General polarization of PLHV1-1 (green), PLHV4-1 (blue), DMPC liposomes (yellow) and S26L14 nanotubes (black) from a Laurdan emission test by changing the temperature from 8 to 42 °C (A), and DSC analysis of PLHV1-1, DMPC liposome and S26L14 nanotube dispersions (B).

This phase-transition of PLHV at 38 °C was attributed to the DMPC domain, because PLHV has phase-separated DMPC and S26L14 domains and the latter domain had no T_m over the temperature range examined. The large T_m shift of 13 °C arises from the small DMPC domain, which is surrounded by the rigid helix bundle domain of S26L14. Researchers have also reported that smaller lipid domain sizes show higher T_m values using various-sized lipid nanodiscs.³⁵⁻³⁶ According to these studies, the T_m shift of 10 °C was because of a loss of cooperativity in the lipids of domains, which was attributed to its small size and the interaction of boundary lipids with the environment of the surrounding domain. We postulate that the additional 3 °C T_m shift arises from the small fraction of peptide that has inserted into the lipid domain or because of the rigidity of the peptide membrane surrounding the lipid domain.

Interestingly, according to the Laurdan test, PLHV4-1 showed a slightly larger shift of the phase-transition temperature when compared with that of PLHV1-1 (Figure 10A). There are two possible models of PLHVs to consider when accounting for this slight phase-transition shift: vesicles with smaller sized lipid domains or a smaller number of lipid domains in the PLHVs. Because the number of domains cannot influence the phase transition, it was concluded that the DMPC domains in PLHV4-1 are smaller than those present in PLHV1-1.

Controlled release.

Fluorescein isothiocyanate-labeled polyethylene glycol (Mw: 2000) (FITC-PEG2K) was encapsulated into PLHVs with a sufficiently high FITC-PEG2K concentration to quench fluorescence of FITC. Loading efficiencies of FITC-PEG2K with DMPC liposomes, PLHV1-1 and PLHV4-1 were 3.9, 7.1 and 5.8%, respectively. FITC-PEG2K release experiments were carried out at 4, 37 and 42 °C. As shown in Figure 11, FITC-PEG2K released as a function of time under a constant temperature. Encapsulation of FITC-PEG2K was maintained for 4 h at 4 °C for all assemblies examined (Figure 11A–C). For DMPC liposomes, more than 70% of FITC-PEG2K was released rapidly at 37 and 42 °C. This is because the DMPC liposomes are in a disordered phase at 37 and 42 °C (Figure 10). In contrast, PLHV1-1 released FITC-PEG2K

only at 42 °C (Figure 11B), and FITC-PEG2K remained encapsulated at 37 °C because this temperature is lower than the T_m . Thus, the DMPC domain acted as a temperature-responsive gate. For PLHV4-1, in a similar manner, FITC-PEG2K was not released at 37 °C. However, at 42 °C, slow release was observed (Figure 11C). Presumably, the smaller DMPC domain size reduced the release rate of FITC-PEG2K from PLHV4-1. Furthermore, another small hydrophilic dye, sulforhodamine B (SRB), also remained trapped inside the nanoparticles at 37 °C and was released at 42 °C from PLHV1-1 and PLHV4-1 (Figure 12). After heating at 42 °C for 4 h, greater release of SRB was observed than that of FITC-PEG2K. These results also support that the lipid domain size can potentially define the size and release rate of trapped material. Therefore, this result indicates that our hybrid vesicle can entrap and release drugs.

The release kinetics of the polymer fluorescein isothiocyanate-labeled polyethylene glycol (Mw: 5000) (FITC-PEG5K), which has a larger molecular weight, was evaluated. The release of FITC-PEG5K from PLHV1-1 was not suppressed at 42 °C (Figure 11D). In contrast, DMPC liposomes leaked FITC-PEG5K equally as FITC-PEG2K at both 37 and 42 °C (Figure 13).

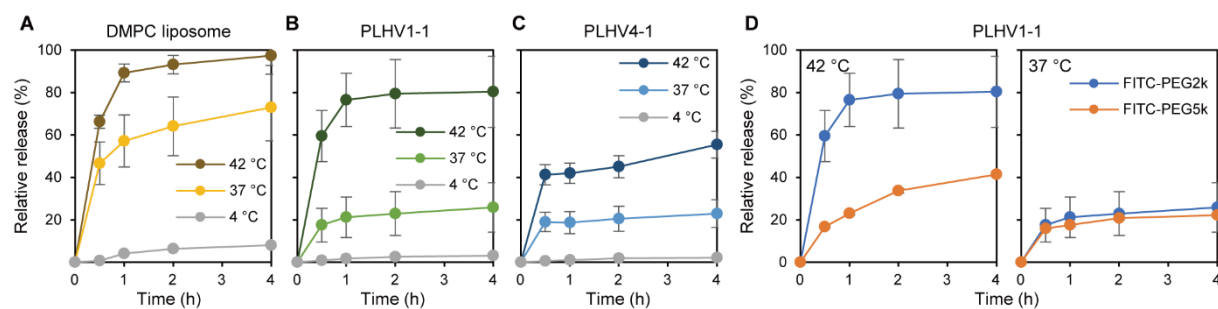


Figure 11. Cumulative release of FITC-PEG2K (Mw: 2000) from DMPC liposomes (A), PLHV1-1 (B) and PLHV4-1 (C) at 4, 37 and 42 °C. The molecular weight (2 and 5 kDa) dependent cumulative release of FITC-PEG from PLHV1-1 at 37 and 42 °C (D).

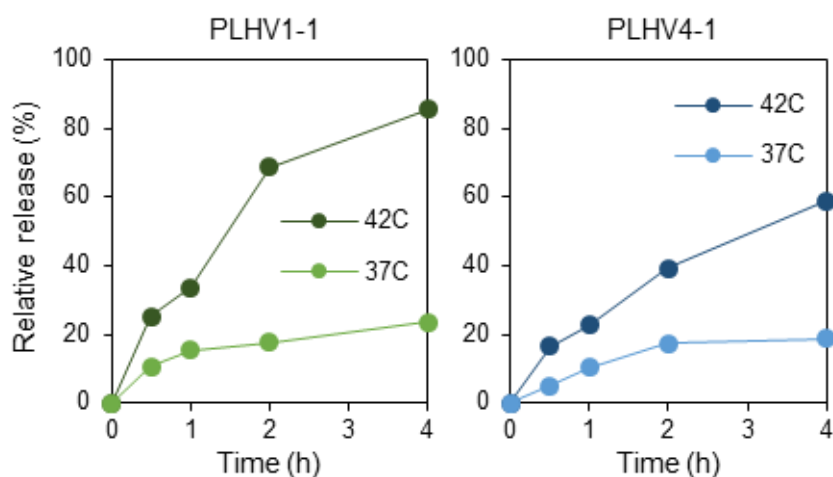


Figure 12. Cumulative release of sulforhodamine B (Mw: 559) from PLHV1-1 and PLHV4-1 at 37 and 42 °C.

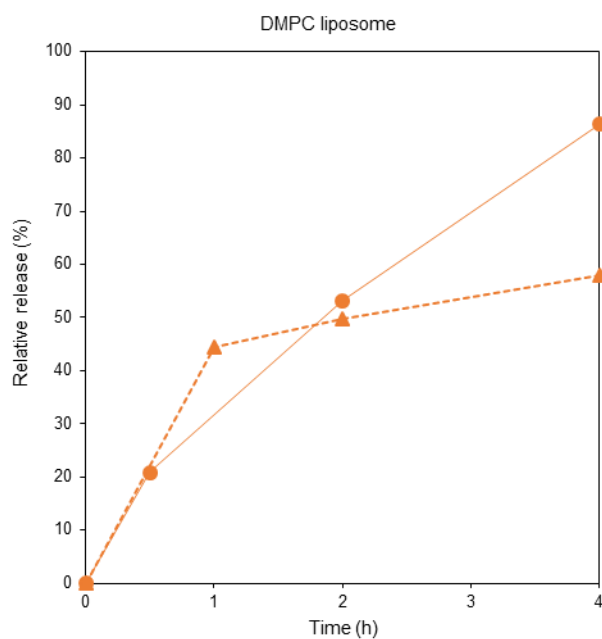


Figure 13. Cumulative release of FITC-PEG5K (Mw: 5000) from DMPC liposomes at 37 (triangle, dot line) and 42 °C (circle, solid line).

Conclusions

PLHVs containing a peptide membrane with a lipid domain were constructed and their morphological stability, phase-separation and phase-transition properties were investigated. FRET analysis revealed the phase-separated structure of PLHVs. The DMPC domain present in PLHVs has a phase-transition temperature of 38 °C, which was shifted due to its small size and the rigidity of the surrounding peptide membrane. Furthermore, PLHV showed rapid release of FITC-PEG2K only at 42 °C, whereas the release rate of FITC-PEG5K was reduced at this temperature. By controlling the size of the lipid domain, on demand size-tuning of size-selective drug release will be possible. The designed peptide-lipid hybrid vesicle and “lipid gate” are a promising tool for smart drug delivery.

References

1. Li, X.; Wang, X. D.; Sha, L. P.; Wang, D.; Shi, W.; Zhao, Q. F.; Wang, S. L., Thermosensitive Lipid Bilayer-Coated Mesoporous Carbon Nanoparticles for Synergistic Thermochemotherapy of Tumor. *Acs Appl Mater Inter* **2018**, 10 (23), 19386–19397.
2. Sercombe, L.; Veerati, T.; Moheimani, F.; Wu, S. Y.; Sood, A. K.; Hua, S., Advances and Challenges of Liposome Assisted Drug Delivery. *Front Pharmacol* **2015**, 6.
3. Allen, T. M.; Cullis, P. R., Liposomal drug delivery systems: From concept to clinical applications. *Adv Drug Deliver Rev* **2013**, 65 (1), 36–48.
4. Akbarzadeh, A.; Rezaei-Sadabady, R.; Davaran, S.; Joo, S. W.; Zarghami, N.; Hanifehpour, Y.; Samiei, M.; Kouhi, M.; Nejati-Koshki, K., Liposome: classification, preparation, and applications. *Nanoscale Res Lett* **2013**, 8, 102.
5. Peer, D.; Karp, J. M.; Hong, S.; Farokhzad, O. C.; Margalit, R.; Langer, R., Nanocarriers as an emerging platform for cancer therapy. *Nature nanotechnology* **2007**, 2 (12), 751–760.

6. Mohammadi, M.; Taghavi, S.; Abnous, K.; Taghdisi, S. M.; Ramezani, M.; Alibolandi, M., Hybrid Vesicular Drug Delivery Systems for Cancer Therapeutics. *Adv Funct Mater* **2018**, 1802136.
7. Beales, P. A.; Khan, S.; Muench, S. P.; Jeuken, L. J. C., Durable vesicles for reconstitution of membrane proteins in bio-technology. *Biochemical Society transactions* **2017**, 45, 15–26.
8. Schulz, M.; Binder, W. H., Mixed Hybrid Lipid/Polymer Vesicles as a Novel Membrane Platform. *Macromol Rapid Comm* **2015**, 36 (23), 2031–2041.
9. Le Meins, J. F.; Schatz, C.; Lecommandoux, S.; Sandre, O., Hybrid polymer/lipid vesicles: state of the art and future perspectives. *Mater Today* **2013**, 16 (10), 397–402.
10. Pippa, N.; Stellas, D.; Skandalis, A.; Pispas, S.; Demetzos, C.; Libera, M.; Marcinkowski, A.; Trzebicka, B., Chimeric lipid/block copolymer nanovesicles: Physico-chemical and bio-compatibility evaluation. *Eur J Pharm Biopharm* **2016**, 107, 295–309.
11. Olubummo, A.; Schulz, M.; Schops, R.; Kressler, J.; Binder, W. H., Phase Changes in Mixed Lipid/Polymer Membranes by Multivalent Nanoparticle Recognition. *Langmuir* **2014**, 30 (1), 259–267.
12. Schulz, M.; Werner, S.; Bacia, K.; Binder, W. H., Controlling Molecular Recognition with Lipid/Polymer Domains in Vesicle Membranes. *Angew Chem Int Edit* **2013**, 52 (6), 1829–1833.
13. Paxton, W. F.; McAninch, P. T.; Achyuthan, K. E.; Shin, S. H. R.; Monteith, H. L., Monitoring and modulating ion traffic in hybrid lipid/polymer vesicles. *Colloid Surface B* **2017**, 159, 268–276.
14. Khan, S.; Li, M. Q.; Muench, S. P.; Jeuken, L. J. C.; Beales, P. A., Durable proteo-hybrid vesicles for the extended functional lifetime of membrane proteins in bionanotechnology. *Chem Commun* **2016**, 52 (73), 11020–11023.
15. Chemin, M.; Brun, P. M.; Lecommandoux, S.; Sandre, O.; Le Meins, J. F., Hybrid polymer/lipid vesicles: fine control of the lipid and polymer distribution in the binary membrane. *Soft Matter* **2012**, 8 (10), 2867–2874.

16. Dao, T. P. T.; Fernandes, F.; Er-Rafik, M.; Salva, R.; Schmutz, M.; Brulet, A.; Prieto, M.; Sandre, O.; Le Meins, J. F., Phase Separation and Nanodomain Formation in Hybrid Poly-mer/Lipid Vesicles. *Acs Macro Lett* **2015**, 4 (2), 182–186.
17. Kowal, J.; Wu, D.; Mikhalevich, V.; Palivan, C. G.; Meier, W., Hybrid Polymer-Lipid Films as Platforms for Directed Mem-brane Protein Insertion, *Langmuir* **2015**, 31, 4868–4877.
18. Al-Ahmady, Z. S.; Al-Jamal, W. T.; Bossche, J. V.; Bui, T. T.; Drake, A. F.; Mason, A. J.; Kostarelos, K., Lipid-Peptide Vesicle Nanoscale Hybrids for Triggered Drug Release by Mild Hyperthermia in Vitro and in Vivo. *Acs Nano* **2012**, 6 (10), 9335–9346.
19. Ueda, M.; Seo, S.; Müller, S.; M., M. R.; Ito, Y., Integrated Nanostructures Based on Self-Assembled Amphiphilic Polypeptides. *American Chemical Society*: **2017**; p 19–30.
20. Ueda, M.; Uesaka, A.; Kimura, S., Selective disruption of each part of Janus molecular assemblies by lateral diffusion of stimuli-responsive amphiphilic peptides. *Chem Commun (Camb)* **2015**, 51 (9), 1601–1604.
21. Ueda, M.; Makino, A.; Imai, T.; Sugiyama, J.; Kimura, S., Versatile peptide rafts for conjugate morphologies by self-assembling amphiphilic helical peptides. *Polym J* **2013**, 45 (5), 509–515.
22. Kanzaki, T.; Horikawa, Y.; Makino, A.; Sugiyama, J.; Kimura, S., Nanotube and Three-Way Nanotube Formation with Nonionic Amphiphilic Block Peptides. *Macromol Biosci* **2008**, 8 (11), 1026–1033.
23. Huang, J.; Bonduelle, C.; Thevenot, J.; Lecommandoux, S.; Heise, A., Biologically Active Polymersomes from Amphiphilic Glycopeptides, *J. Am. Chem. Soc.* **2012**, 134, 119–122.
24. Ueda, M.; Makino, A.; Imai, T.; Sugiyama, J.; Kimura, S., Rational design of peptide nanotubes for varying diameters and lengths. *J Pept Sci* **2011**, 17 (2), 94–99.
25. Kaindl, T.; Adlkofer, K.; Morita, T.; Umemura, J.; Kononov, O.; Kimura, S.; Tanaka, M., Modulation of Band Bend-ing of Gallium Arsenide with Oriented Helical Peptide Monolayers. *J Phys Chem C* **2010**, 114 (51), 22677–22683.

26. Nakano, M.; Fukuda, M.; Kudo, T.; Miyazaki, M.; Wada, Y.; Matsuzaki, N.; Endo, H.; Handa, T., Static and Dynamic Properties of Phospholipid Bilayer Nanodiscs. *J Am Chem Soc* **2009**, 131 (23), 8308–8312.
27. Lewis, B. A.; Engelman, D. M., Lipid Bilayer Thickness Varies Linearly with Acyl Chain-Length in Fluid Phosphatidylcholine Vesicles. *J Mol Biol* **1983**, 166 (2), 211–217.
28. Kornilova, A. Y.; Wishart, J. F.; Xiao, W. Z.; Lasey, R. C.; Fedorova, A.; Shin, Y. K.; Ogawa, M. Y., Design and characterization of a synthetic electron-transfer protein. *J Am Chem Soc* **2000**, 122 (33), 7999–8006.
29. Cohen, C.; Parry, D. A. D., Alpha-Helical Coiled Coils and Bundles - How to Design an Alpha-Helical Protein. *Proteins* **1990**, 7 (1), 1–15.
30. Parasassi, T.; Krasnowska, E. K.; Bagatolli, L.; Gratton, E., LAURDAN and PRODAN as polarity-sensitive fluorescent membrane probes. *J Fluoresc* **1998**, 8 (4), 365–373.
31. Parasassi, T.; Gratton, E., Membrane lipid domains and dynamics as detected by Laurdan fluorescence. *J Fluoresc* **1995**, 5 (1), 59–69.
32. Parasassi, T.; De Stasio, G.; Ravagnan, G.; Rusch, R. M.; Gratton, E., Quantitation of Lipid Phases in Phospholipid-Vesicles by the Generalized Polarization of Laurdan Fluorescence. *Biophys J* **1991**, 60 (1), 179–189.
33. Bakht, O.; Pathak, P.; London, E., Effect of the structure of lipids favoring disordered domain formation on the stability of cholesterol-containing ordered domains (lipid rafts): Identification of multiple raft-stabilization mechanisms. *Biophys J* **2007**, 93 (12), 4307–4318.
34. Viard, M.; Gallay, J.; Vincent, M.; Meyer, O.; Robert, B.; Paternostre, M., Laurdan solvatochromism: Solvent dielectric relaxation and intramolecular excited-state reaction. *Biophys J* **1997**, 73 (4), 2221–2234.
35. Denisov, I. G.; McLean, M. A.; Shaw, A. W.; Grinkova, Y. V.; Sligar, S. G., Thermotropic phase transition in soluble nanoscale lipid bilayers. *J Phys Chem B* **2005**, 109 (32), 15580–15588.

- 36 Shaw, A. W.; McLean, M. A.; Sligar, S. G., Phospholipid phase transitions in homogeneous nanometer scale bilayer discs. *Febs Lett* **2004**, 556 (1-3), 260–264.

Chapter 3

Tubular network composed of a mixture of amphiphilic polypeptides having different hydrophilic blocks

Introduction

According to the blood vessels¹⁻³, endoplasmic reticulum⁴⁻⁶, mitochondria^{7,8} and Golgi apparatus⁹⁻¹¹ in the living body, the usefulness of the combination of tubular structures and networks structure has been shown. Tubular networks are promising tool as biomaterial owing to the large surface area and as tracts due to the tubular structure. However, so far, only studies to elucidate its structure formation mechanism^{4,7} and relationship between the morphology and functions^{2,9} have been reported. Thus, in order to apply these tubular network structures as biomaterials, the creation of artificial tubular network is important research. Here, researches on network structure has been highly reported in the gel design field. However there has been few reports showing preparation of artificial tubular network^{12,13}. Lipids make the use of its membrane flexibility to extend the tube from the cell membrane to form a network of tubes¹⁴⁻¹⁶. However, lipid-based networks are very unstable and difficult to apply to materials. Therefore, we aimed the network structure by controlling two factors of stability and flexibility.

We have succeeded to prepare the rigid nanotubes having a uniform diameter by using amphiphilic polypeptide, SL12¹⁷⁻²⁰. This SL12 nanotube was very stable structurally because it maintained the structure for at least 6 months. In the previous report, it was cleared that the hydrophobic helical block of SL12 was important factor to create the rigid nanotube morphology. In this research, we focused on amphiphilic polypeptide having the same hydrophobic block as SL12 and different hydrophilic chain of polyethylene glycol (PEG) which was expected to be more flexible than polysarcosine due to its lower density of polymer. By combining the flexible and unstable PL12 nanotube with rigid SL12 nanotube, it was expected that the fusion among their nanotubes and the development of branched tubular network.

Experimental Section

Materials. All amino acids and condensation reagents were purchased from Watanabe Chemical Ind., Ltd., Japan.

Preparation of molecular assemblies. Polypeptides (20 mg) and lipids (20 mg) were dissolved in ethanol (400 μ l) as a stock solution. An aliquot of the peptide and lipid stock solution were injected into a saline (1 mL) while stirring. After stirring for 30 min, this dispersion was heated at 90 °C for 1 h. For compositions with polypeptides and lipid, the stock ethanol solutions of the amphiphilic polypeptides were mixed to obtain total 10 μ L of the mixture with the desired ratio before injection into saline. The mixture solution was then injected and heated in the same manner.

Transmission electron microscopy (TEM). TEM images were taken using a JEOL JEM-1230 at an accelerating voltage of 80 kV. For the observation, a drop of dispersion was mounted on a carbon-coated Cu grid (Okenshoji Co., Ltd., Japan) and stained negatively with 2% samarium acetate, followed by suction of the excess fluid with a filter paper.

Dynamic light scattering (DLS). The hydrodynamic diameter of molecular assemblies in saline was analyzed by DLS-8000KS (Photal Otsuka Electronics) using a He-Ne laser. All measurements were performed at 25 °C.

Circular Dichroism (CD). CD measurements were carried out on a JASCO J-720 (JEOL, Japan) using a cell with an optical path length of 1 cm. Data was recorded at 25 °C. 0.35 mM peptide was used for self-assembly in saline, and the dispersion was diluted five-fold before CD data collection.

Fluorescent Spectroscopy. The fluorescent spectra of assembled dispersions were obtained using a JASCO FP-6500 spectrofluorometer at 25 °C with a transmission cell.

Laurdan Test. The membrane fluidity of PLHVs, S26L14 nanotubes and DMPC liposomes were measured with *N,N*-dimethyl-6-dodecanoyl-2-naphthylamine (Laurdan). Laurdan is a fluorescent dye that is sensitive to the polarity of its surrounding environment. A general polarization value, GP_{340} , was calculated: $GP_{340} = (I_{440} - I_{490}) / (I_{440} + I_{490})$, where I_{440} and I_{490} are emission intensities at 440 and 490 nm of excited Laurdan at 340 nm. The temperature range of 10–42 °C was controlled by a circulating water bath.

Membrane fluidity. The membrane fluidity of hybrid vesicle, peptide nanotube and DMPC liposomes were measured using 1,6-diphenyl-1,3,5-hexatriene (DPH). By using fluorescence spectrophotometer FP-6500 (JASCO, Tokyo, Japan), the hybrid vesicles or peptide nanotube or DMPC liposome containing DPH polarization were measured. 10 μ L of 100 μ M ethanol solution of DPH was incorporated into 0.25 mM assembly dispersion. Samples were incubated for 30 min in the dark before the experiment. Excitation and emission wavelength were set to 360 and 430 nm, respectively. Polarized light was excited vertically and emission light was recorded as both perpendicular, I_{\perp} (0°, 0°) and parallel, I_{\parallel} (0°, 90°). The polarization (P) of DPH was calculated as follows; $P = (I_{\parallel} - GI_{\perp}) / (I_{\parallel} + GI_{\perp})$, $G = I_{\perp} / I_{\parallel}$. I_{\perp} and I_{\parallel} are emission intensities perpendicular (90°, 0°) and parallel (90°, 90°) respectively to the horizontally polarized light. G is correction factor. DPH membrane fluidities of different samples were recorded at 10-42 °C.

Synthesis of PL12. The synthesis of PL12 was performed by synthetic scheme in Figure 1A. The hydrophobic 12-mer peptide, H-(L-Leu-Aib)₆-OMe, was synthesized by the conventional liquid phase method²⁰. mPEG (Mw: 750) was used for an initial compound. para-nitrophenyl chlorocarbonate (1.45 g, 7.2 mmol) and triethylamine (1 mL, 7.2 mmol) were added to mPEG (2.7 g, 3.6 mmol) in THF (50 mL) and the mixture was stirred at room temperature for 4 days. After 4 days, the solvent was removed by evaporation and then the solid was purified through sephadex LH-20 column with CHCl₃/MeOH as an eluent solvent. After evaporation, white solid compound **2** (mPEG-pNP) (3.12 g) was obtained.

mPEG-pNP **2** (220 mg) and H-(L-Leu-Aib)₆-OMe (100 mg) were dissolved into DMF (4 mL) and then this mixture was stirred for 4 hours. After that, the solvent was evaporated and the solid was purified through sephadex LH-20 with methanol as an eluent solvent. After evaporation, target compound **3** (PL12) was obtained.

mPEG-pNP **2**: ¹H NMR (400 MHz, DMSO-d₆): δ (ppm) 8.32 (d, 2H, OCCHCHCNO₂ of phenyl group), 7.57 (d, 2H, OCCHCHCNO₂ of phenyl group), 4.36 (t, 2H, CH₃OCH₂CH₂O), 3.59 (t, 2H, CH₃OCH₂CH₂O), 3.52 (m, 71H, OCH₂CH₂O, CH₃O), 3.24 (t, 4H, OCH₂CH₂OCOO). MALDI-TOF MS; calcd. for C₄₂H₇₅NO₂₂ [M + Na]⁺: 968.49, found.: 968.43.

PL12 **3**: ¹H NMR (400 MHz, MeOH-d₄): δ (ppm) 8.08–7.72 (m, 12H, amide), 4.86–4.02 (m, 6H, LeuC^αH), 3.75–3.61 (m, 68H, OCH₂CH₂O), 3.53 (s, 3H, OCH₃), 1.82–1.50 (m, 54H, LeuCH₂, LeuCH, AibCH₃), 1.00–0.85 (m, 36H, LeuCH₃). MALDI-TOF MS; calcd. for C₉₇H₁₈₂N₁₂O₃₂ [M + Na]⁺: 2050.31, found.: 2050.13.

Synthesis of SL12. Amphiphilic polypeptide of polysarcosine₂₆-*b*-(L-Leu-Aib)₆ (SL12) was synthesized as reported previously¹⁻². The syntheses of all compound were confirmed by ¹H NMR spectroscopy and MALDI-TOF MS spectrometry.

Results and Discussion

Effect of hydrophilic chains

PEG-*b*-(L-Leu-Aib)₆ (PL12) was synthesized with mPEG (Mw: 750) and synthesized hydrophobic polypeptide, (L-Leu-Aib)₆ by the scheme in Figure 1A. PL12 was identified by MALDI-TOF mass and ¹H NMR measurements to confirm that PL12 had successfully PEG block with the molecular weight of 750, which was a 17-mers (Figure 1). SL12 was obtained by the polysarcosine extension at *N*-termini of (L-Leu-Aib)₆. MALDI-TOF mass and NMR

spectra showed the degree of polymerization of 21. The length of hydrophilic block was almost same between PL12 and SL12.

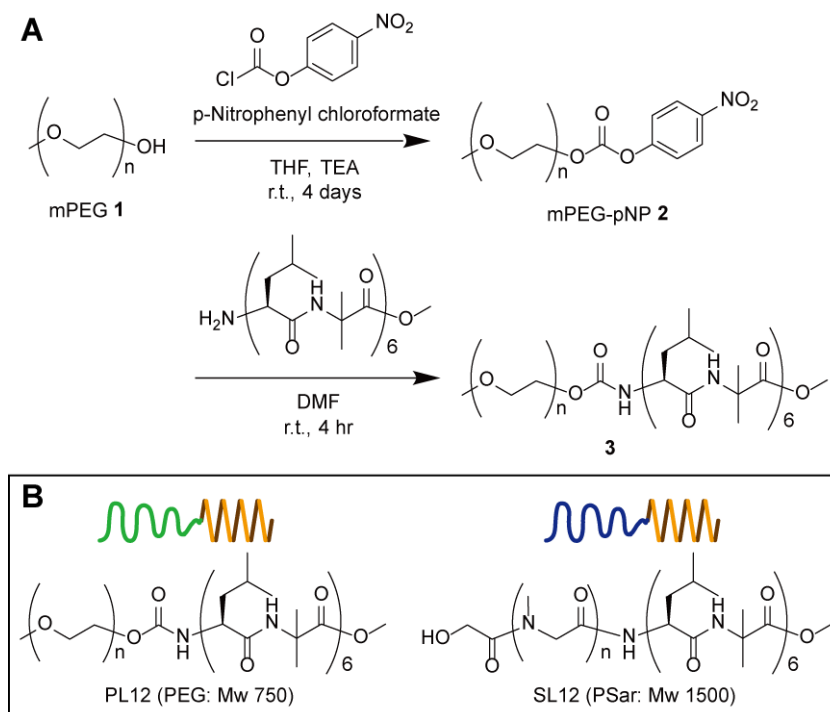


Figure 1. Synthetic scheme of PL12 (A) and chemical structure of PL12 and SL12 (B).

The secondary structures of PL12 and SL12 were evaluated by CD spectra (Figure 2). Both of PL12 and SL12 showed α -helix structure in ethanol. This helical structure corresponded to folding of hydrophobic block because PEG and polysarcosine were random chains. PEG block didn't affect the folding of hydrophobic block. All difference among PL12 and SL12 was only kinds of hydrophilic polymers.

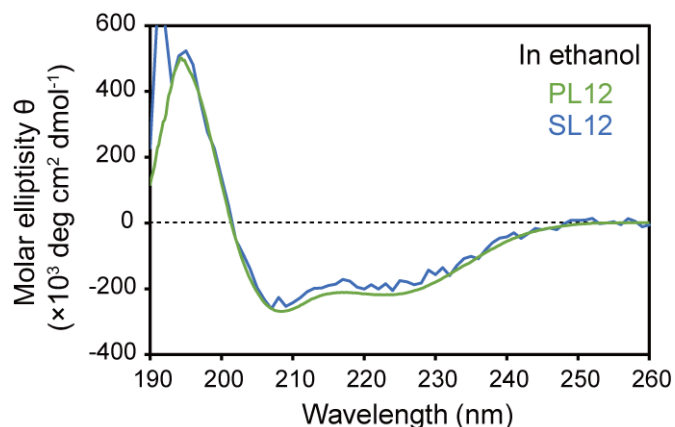


Figure 2. CD spectra of PL12 (green) and SL12 (blue) in ethanol.

The morphology of assemblies prepared from PL12 and SL12 were observed by transmission electron microscopy (TEM) (Figure 3 and Table 1). These assemblies were prepared by the ethanol injection method and heat treatment at 90 °C for 1 h. A tubular assembly with a uniform diameter of 80 nm was obtained in the both case. This diameter of 80 nm was dominated by a membrane curvature which comes from a tilted packing of amphiphilic polypeptides between neighbor helices^{17,21}. This was reasonable because PL12 and SL12 had the same hydrophobic α -helical block. However, the length of nanotube was largely different between PL12 and SL12 nanotubes. SL12 nanotube had a length of 200 nm, which was reported previously¹⁷⁻²⁰. On the contrary, the length of PL12 nanotube had a wide distribution of 500–10,000 nm.

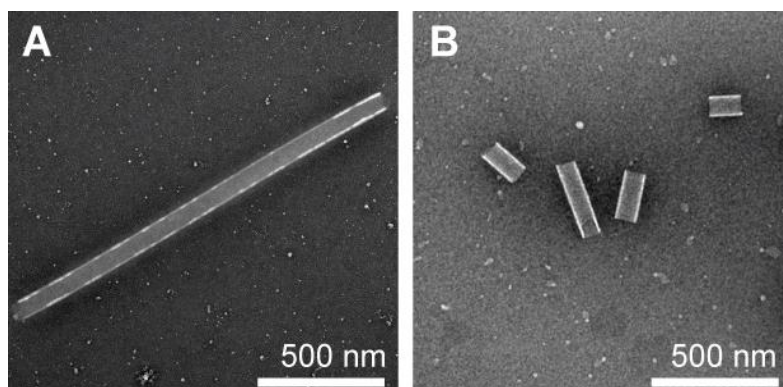


Figure 3. TEM images, negatively stained by 1% samarium acetate, of molecular assembly prepared from PL12 (A) and SL12 (B) in saline.

Table 1. Characterization of molecular assembly prepared from PL12 and SL12 by ethanol injection method and heat treatment at 90 °C for 1 h.

Amphiphile	Shape	Diameter (nm)	Length (nm)	Hydrodynamic diameter (nm)	P	GP ₃₄₀
PL12	nanotube	80	500–10000	7933	0.25	0.24
SL12	nanotube	80	100–400	155	0.41	0.36

By increasing time of heat treatment, SL12 nanotube elongated moderately to ca.500 nm but PL12 nanotube grew drastically to more than 10 μm (Figure 4). Average hydrodynamic diameter from DLS measurement also showed that quick and slow elongation of PL12 and SL12 nanotubes (Figure 4I). These results suggest that SL12 nanotube were enough stable morphologically and PL12 nanotube had a trend to fuse to neighbor nanotube one by one.

Next, the membrane fluidity and polarity of nanotubes prepared from PL12 and SL12 were estimated by using 1,6-diphenyl-1,3,5-hexatriene (DPH)²²⁻²⁴ and *N,N*-dimethyl-6-dodecanoyl-2-naphthylamine (Laurdan)²³⁻²⁵, respectively (Table 1). The polarization (*P*) of

DPH in PL12 and SL12 nanotubes showed 0.25 and 0.41, which meant that PL12 membrane was slightly more fluid than SL12 membrane in assembly. Furthermore, general polarity (GP_{340}) of Laurdan in PL12 and SL12 nanotubes were 0.24 and 0.36. These results indicated that, compared with polysarcosine brush layer, PEG brush layer was easy to permeate water molecules because this GP_{340} value reflected a membrane polarity, which was amount of water molecule invading around Laurdan reagents in the hydrophobic layer. The lower density of PEG than polysarcosine on assembly may permeate more water molecules. Furthermore, it is hypothesized the water invasion makes the membrane fluid and unstable by disturbing a hydrophilic-hydrophobic interface, resulting in the trend of quick elongation of PL12 nanotube which is induced by fusion among the open edges of PL12 nanotube.

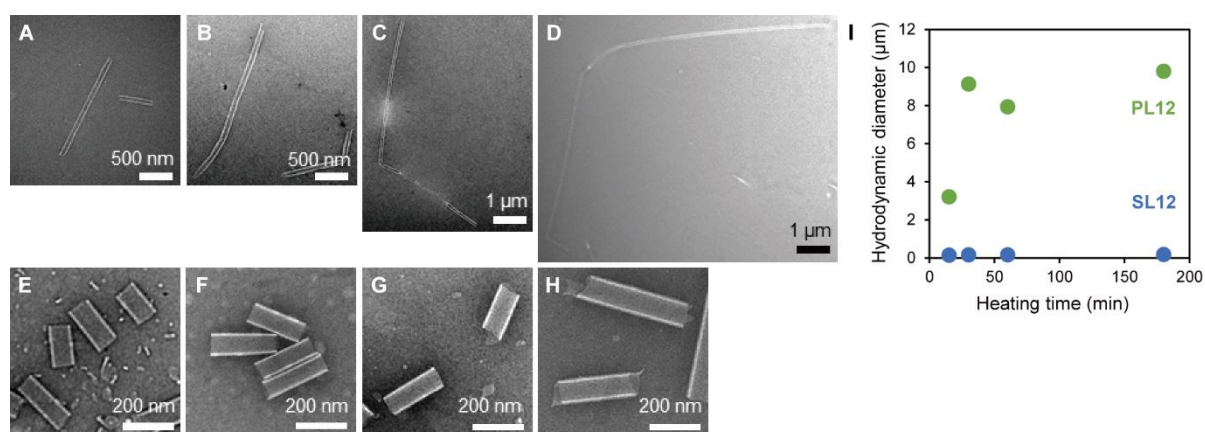


Figure 4. TEM images (A-H) and hydrodynamic diameter (I) of nanotubes from PL12 and SL12 after heat treatment at 90 °C for 10 (A, E), 30 (B, F), 60 (C, G) and 180 min (D, H).

Tubular network

The morphology of assemblies prepared from a combination of PL12 and SL12 at various mixing ratios were observed by TEM (Figure 5). TEM observation showed that a mixture of PL12 and SL12 at mixing ratio of 4:6, 3:7, 2:8 and 1:9 formed the same tubular

Tubular network composed of amphiphilic polypeptides

assembly as SL12 nanotube having 80 nm diameter and 200–400 nm length (Figure 5F-I). Actually, size from DLS measurement also be the same in these co-assemblies (Figure 5J). Furthermore, CD spectra indicated that the secondary structure of constituent amphiphiles and helix bundle content among amphiphiles, which was shown as a ratio of $\theta_{222}/\theta_{208}$ were no different (Figure 5K). From DPH test, the fluidity of these mixture membrane was the same as that of pure SL12 membrane (Figure 5L). These results show that SL12 can be dominant for the morphology of co-assembly in these SL12-rich ratio even if PL12 molecule inserts SL12 membrane. These co-assemblies acted as a stable structure like SL12 nanotube because rich polysarcosine brushes covered enough the hydrophobic layer.

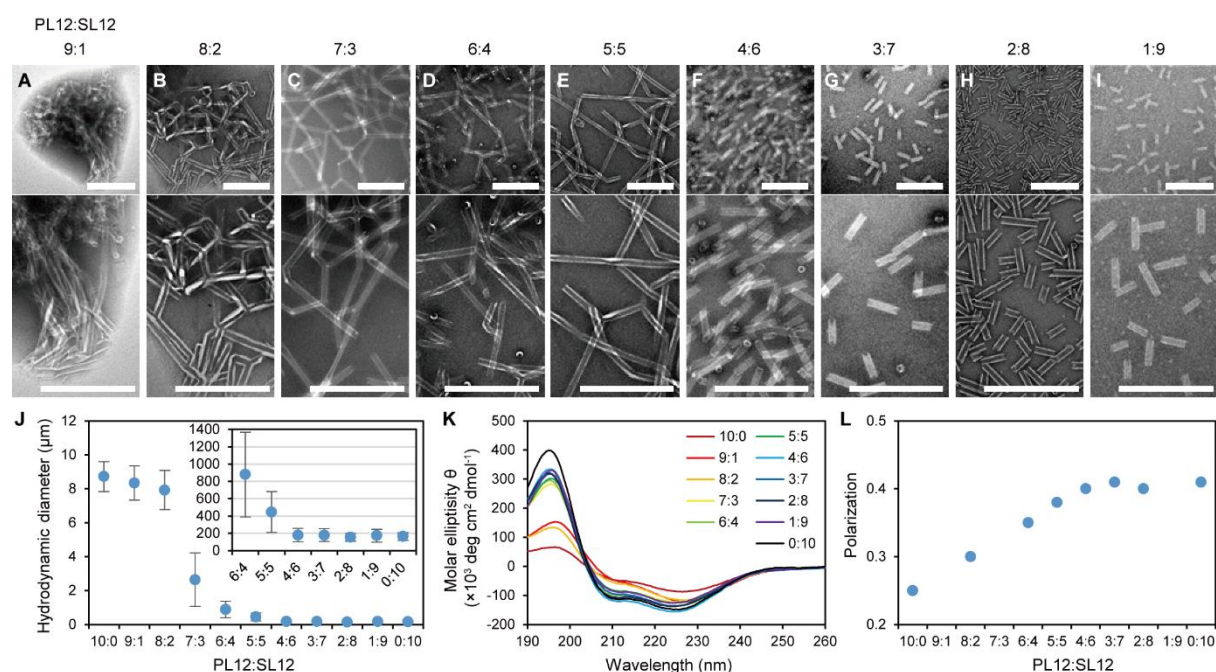


Figure 5. TEM images (A–I), hydrodynamic diameter (J), CD spectra (K) and membrane fluidity (L) of molecular assemblies prepared from a mixture of PL12 and SL12 with various ratio of 9:1, 8:2, 7:3, 6:4, 5:5, 4:6, 3:7, 2:8 and 1:9 (A–I). Scale bars are 1 μm. Hydrodynamic diameter and membrane fluidity were measured by DLS measurement and by DPH, respectively.

On the other hand, when PL12 was mixed with SL12 in PL12-rich mixing ratios (5:5, 6:4, 7:3, 8:2 and 9:1), tubular networks were observed (Figure 5A-E). The shape of tubular network looked to be composed of fused nanotubes between their open edges because the uniform diameter of 80 nm diameter was the same as diameter of nanotube prepared from a single component of PL12 and SL12, and the membrane thickness of tubular network also be similar to that of PL12 and SL12 nanotubes. More and more PL12 content, longer and longer network was observed in TEM images. Hydrodynamic diameter from DLS analysis supported that tubular networks of mixing ratio of 9:1 and 8:2 (PL12:SL12) were larger than those of the ratios of 7:3, 6:4 and 5:5 (Figure 5J). This result corresponds to the trend that PL12 nanotube quickly fuses to elongate (Figure 4). Actually, more PL12 content made the co-assembled membrane more fluid (Figure 5L) and might accelerate a fusion between the open edges of nanotubes. The ratio $\theta_{222}/\theta_{208}$, which was enough higher than 1, of CD spectra indicated that too excess PL12 content of assembly induced an aggregation of tubular network in the case of mixing ratios; 10:0, 9:1 and 8:2 (Figure 5K). Interestingly, pure PL12 formed not tubular network but linear nanotube. By co-assembling with PL12 and SL12, nanotube fused between several nanotubes, resulting that branched nanotube was obtained. Thus, the reasons to form network were not only higher membrane fluidity and lower stability. Co-assembling may enable a complex morphological formation mechanism.

This co-assembled tubular network was developed on time of heat treatment (Figure 6A-F). Nanotubes fused to other nanotubes between the open edges, resulting in tubular network formation. Relative proportion of linear and branched junction on tubular network were summarized in Figure 6G. Linear and branched junction was fused region between two nanotubes and between more than three nanotubes, respectively (Figure 6H). The number of branched junction was increased by heating for more than 30 min. After 30 min, the ratio of linear and branched junction were kept. On the other hand, number of composed nanotube on one network was summarized in Figure 6I. The number also was increased by heating longer and longer. Thus, increasing the branched junction and the number of composed nanotube developed tubular network widely.

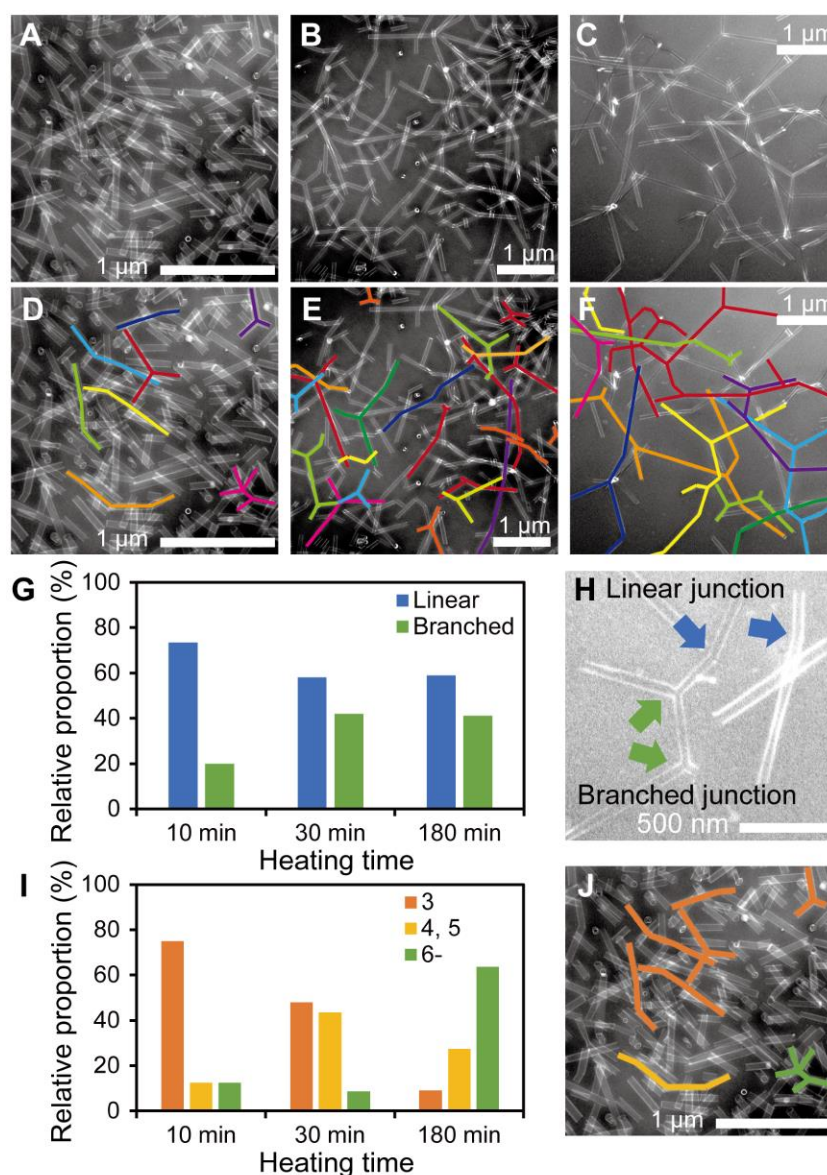


Figure 6. TEM images of tubular network prepared from a mixture of PL12 and SL12 with molar ratio of 1:1 after heat treatment at 90 °C for 10 min (A, D), 30 min (B, E) and 180 min (C, F). Color lines showing the tubular network from more than three tubular parts (D-F). Relative proportion and TEM image of linear and branched junction on tubular network containing more than three tubular parts (G and H). Blue and green arrow represent linear junction between two tubular parts and branched junction between more than three tubular parts (H). Relative proportion and TEM image of constituent number of tubular parts (I and J).

Conclusions

The nano- and micro-ordered tubular network is a promising tool in various fields involving a tissue engineering. By co-assembling with two types of amphiphilic polypeptides, PL12 and SL12, tubular network was produced. This tubular network was prepared by fusion between several nanotubes. Furthermore, the heat treatment increased the branched junctions among nanotubes and the number of constituent nanotubes of network, resulting that the tubular network was developed widely. Under developing the network, the uniform diameter and membrane thickness were maintained. This report opened up the possibility to control artificial tubular network

References

1. Toi, M.; Asao, Y.; Matsumoto, Y.; Sekiguchi, H.; Yoshikawa, A.; Takeda, M.; Kataoka, M.; Endo, T.; Kawaguchi-Sakita, N.; Kawashima, M.; Fakhrehajani, E.; Kanao, S.; Yamaga, I.; Nakayama, Y.; Tokiwa, M.; Torii, M.; Yagi, T.; Togashi, K.; Shiina, T. *Scientific Reports*, **2017**, 7, 41970.
2. Chappell, C. J.; Wiley, M. D.; Bault L. V. *Cells Tissues Organs*, **2011**, 195, 94-107,
3. Geudens, I.; Gerhardt, H.; *Development*, **2011**, 138, 4569-4583.
4. Powers, E. R.; Wang, S.; Liu, Y. T.; Rapoport, A. T. *Nature*, **2017**, 543, 257-260.
5. Voeltz, K. G.; Prinz, A. W.; Shibata, Y.; Rist, M. J.; Rapoport, A. T. *Cell* 2006, 124, 573-586.
6. Georgiades, P.; Allan, J. V.; Wright, D. G.; Woodman, G. P.; Udommai, P.; Chung, A. M.; Waigh, A. T.; *Scientific Reports*, **2017**, 7, 16474.
7. Rambold, S. A.; Kostecky, B.; Elia, N.; Lippincott-Schwartz, J. *Proc. Nat. Acad. Sci.* **2011**, 108, 10190-10195.
8. Rafelski, M. S. *BMC Biology*, **2013**, 11, 71

Tubular network composed of amphiphilic polypeptides

9. Trucco, A.; Polishchuk, S. R.; Martella, O.; Pentima, D. A.; Fusella, A.; Giandomenico, D. D.; Pietro, S. E.; Beznoussenko, V. G.; Polishchuk, V. E.; Baldassarre, M.; Buccione, R.; Geerts, C. J. W.; Koster, J. A.; Burger, J. N. K.; Mironov, A. A.; Luini, A. *Nat. Cell Biol.*, **2004**, 6, 1071-1081.
10. Mollenhauer, H. H.; Morre, D. J. *Histochem. Cell Biol.*, **1998**, 109, 533-543.
11. Rambourg, A. D.; Clermont, Y.; Ovtracht, L.; Kepes, F. *Molecular and Cellular Biology*, **1995**, 243, 283-293.
12. Kouwer, J. H. P.; Koepf, M.; Sage, L. A. A. V.; Jaspers, M.; Buul, V. M. A.; Elsteen-Akeroyd, H. Z.; Woltinge, T.; Schwartz, E.; Kitto, J. H.; Hoogenboom, R.; Picken, J. S.; Nolte, M. J. R.; Mendes, E.; Rowan, E. A. *Nature*, **2013**, 493, 651-655.
13. Feig, R. V.; Tran, H.; Lee, M.; Bao, Z. *Nat. Commun.*, **2018**, 9, 2740.
14. Zhang, X.; *Scientific Reports*, **2015**, 5, 16559.
15. Simunovic, M.; Mim, C.; Marlovits, C. T.; Resch, G.; Unger, M. V.; Voth, A. G. *Biophys. J.* **2013**, 105, 711-719.
16. Bi, H.; Han, X. *Biotechnology*, **2013**, 2, 7.
17. Ueda, M.; Seo, S. Y.; Nair, G. B.; Muller, S.; Takahashi, E.; Arai, T.; Iyoda, T.; Fujii, S.; Tsuneda, S.; Ito, Y. *ACS Nano*, **2019**, DOI:10.1021/acsnano.8b06189
18. Ueda, M.; Makino, A.; Imai, T.; Sugiyama, J.; Kimura, S. *Soft Matter*, **2011**, 7, 4143-4146.
19. Ueda, M.; Makino, A.; Imai, T.; Sugiyama, J.; Kimura, S. *Chem. Commun.*, **2011**, 47, 3204-3206.
20. Kanzaki, T.; Horikawa, Y.; Makino, A.; Sugiyama, J.; Kimura, S. *Macromol. Biosci.*, **2008**, 8, 1026-1033.
21. Itagaki, T.; Nobe, W.; Uji, H.; Kimura, S., *Chem. Lett.*, **2018**, 47, 726-728.
22. Aleman, C.; Annereau, J-P.; Liang, X-J.; Cardarelli, O. C.; Taylor, B.; Yin, J. J.; Aszalos, A.; Gottesman, M. M., *Cancer Research*, **2003**, 63, 3084-3091.
23. Hirose, M.; Ishigami, T.; Suga, K.; Umakoshi, H., *Langmuir*, **2015**, 31, 12968-12974.
24. Suga, K.; Umakoshi, H. *Langmuir*, **2013**, 29, 4830-4838.

25. Parasassi, T.; Stasio, D. G.; Ravagnan, G.; Rusch, M. R.; Gratton, E., *Biophys. J.*, **1991**, 60. 179-189.

Tubular network composed of amphiphilic polypeptides

Chapter 4

Concluding Remarks

Concluding Remarks

This section briefly summarizes the results of investigation on the preparation, characterization, and morphological analysis of hybrid molecular assemblies composed of amphiphilic polypeptides having a hydrophobic helical segment with other amphiphiles.

Chapter 1 describes the general introduction on the self-assembled structures made of amphiphilic polypeptides and the composite with other components. Amphipathic polypeptides having a helical structure in the hydrophobic part were designed and the morphology of their assembled structures was investigated. In addition, the effect of conjugation with same type of amphiphilic polypeptide having different length of hydrophobic helix and with different types of amphiphilic molecules such as amphiphilic polypeptide having PEG, and phospholipids was also investigated. First a helical structure-forming hydrophobic sequence composed of leucine- and aminoisobutyric acid-alternating sequence was conjugated with PSar. When the hydrophobic part composed of 8 residues conjugated with PSar (SL8), it formed a 3_{10} helix structure. When it composed of 12 (SL12) and more (SL14, SL16, SL18, and SL20), they formed an α -helix structure. Transmission electron microscope (TEM) observation showed that SL8 formed a fiber structure and SL12, SL14, SL16, SL18 and SL20 had a sheet-based structure (SL12, SL14: tube, SL16: vesicle, SL18, SL20: sheet). The tube and vesicle were considered to be formed by rolling sheet up. The parameters affecting the structures of tubes, vesicles and sheets in the assemblies of SL12 to SL20 was discussed and the different packing pattern and interaction between the neighbor helices was also considered. Next, co-assembly of SL12 and SL16 was prepared. It did not form a homogeneous miscible membrane but formed a co-assembled structure composed of a phase-separated membrane. TEM observation showed the SL12 tube was capped with the L16 vesicle. Second, in order to investigate the influence of the hydrophilic part, the hydrophobic part composed of 12 residues was conjugated with PEG (PL12). Like SL12 with PSar, TEM observation showed nanotube structure with a diameter of 80 nm was formed. This result demonstrated that the influence of hydrophilic part on the assembly shape was not so large as hydrophobic helical block, and that the hydrophobic helix determined the assembled structure. Thirdly, co-assembly with phospholipids was performed and it formed phase-separated membrane composed of polypeptides and phospholipids.

In Chapter 2, based on the findings in Chapter 2, the phase-separated co-assembly of phospholipids and amphiphilic polypeptides was developed. The co-assembly had a temperature-responsive drug release ability. A mixture of amphiphilic polypeptide SL14 and phospholipid 1,2-dimyristoyl-sn-glycero-3-phosphocholine (DMPC) formed a 75 nm diameter co-assembled vesicle (peptide-lipid hybrid vesicle (PLHV)) in saline at a mixing ratio of 4:1 to 1:1 (SL14:DMPC), which was confirmed by TEM observation and dynamic light scattering (DLS) measurement. Spectroscopic analysis using the fluorescence resonance energy transfer (FRET) phenomenon revealed that PLHV was composed of a phase-separated membrane with independent peptidic and lipidic membranes, not a homogeneous miscible membrane of them. The lipid domain in PLHV showed the phase-transition behavior similar to liposome composed of pure lipid membrane. The phase-transition temperature of PLHV was 38 °C, which was higher than the phase-transition temperature (25 °C) of the pure DMPC membrane. This shift was considered to be induced by the smaller size of the lipid domain and surrounding of lipid membrane with the robust peptide membrane. Because PLHV was a closed structure, it can encapsulate hydrophilic molecules, retain them at 37 °C, and show the release of them at 42 °C. Lipid domain in PLHV worked as a temperature-responsive gate. The possibility of controlling the release rate of inclusion depending on the size of the lipid membrane was also suggested.

Chapter 3 summarized the research on hybrid tubular network structure formation by co-assembling PL12 and SL12. As shown in Chapter 2, both PL12 and SL12 formed nanotubes, but the elongation (fusion) speeds of their nanotubes by heating were different from each other. When the membrane fluidity of their nanotubes was measured, PL12 membrane was more fluidic than the SL12 membrane, because a lot of water molecules invaded to the hydrophilic/hydrophobic interface of PL12. This was considered to affect the difference in elongation rates. When PL12 and SL12 were co-assembled at the mixing ratio of 7:3, 6:4, and 5:5 (PL12:SL12), they formed three-way open ends and formed tubular network as a result. Excessive amount of PL12 was considered to promote the network formation because of the higher fluidity.

Concluding Remarks

Chapter 4 summarizes the conclusion obtained in this research and describes future research developments of self-assembled amphiphilic polypeptide with other components.

As demonstrated in the present thesis, the molecular assemblies, which are composed of amphiphilic polypeptides having a hydrophobic helical segment, show unique morphologies and properties, which are accompanied by complex formation between the peptide and lipid that produced highly stable temperature sensitive DDS carrier which controlled and modulate the drug release through lipid block (domain) upon mild hyperthermia. In contrast, tubular network formed by suitable mixture of PL12 and SL12 where hydrophilic block is different. The PL12 may play the major role to form uniform tubular networks. So, helical peptides and different components formed hybrid assemblies through membrane fusion due to the membrane fluidity, and phase separation in assembled membranes. With all these notable points for preparations of molecular assemblies, the author successfully demonstrates a new aspect of molecular assembly of more complex morphology, which is named as “Interesting hybrid assemblies (vesicles and networks)”. The author therefore believes that the important findings of this thesis should be of interest not only for materials scientists and supramolecular chemists but also for many scientists in other fields of medical chemistry, organic chemistry, and biological chemistry, pharmaceuticals and so on.

List of Publications

Chapter 1 “Integrated Nanostructures Based on Self-Assembled Amphiphilic Polypeptides”

Motoki Ueda, Stefan Müller, Siyoong Seo, Md. Mofizur Rahman, and Yoshihiro Ito

Advances in Biospired and Biomedical Materials, volume 1, 2017, 19–30. ed by Yoshihiro Ito, Xuesi Chen and Inn-Kyu Kang, American Chemical Society

Chapter 2 “Spontaneous Formation of Gating Lipid Domain in Uniform-Size Peptide Vesicles for Controlled Release”

Md. Mofizur Rahman, Motoki Ueda, Takuji Hirose, and Yoshihiro Ito

J. Am. Soc. Chem. **2018**, 140, 17956–17961.

Chapter 3 “Tubular network composed of a mixture of amphiphilic polypeptides having different hydrophilic blocks”

Motoki Ueda, Md. Mofizur Rahman, Kon Son, Takuji Hirose, and Yoshihiro Ito

Under preparation

Other Publications

“Spontaneous formation of gating lipid-domain in uniform-size peptide vesicle for control release”

Md. Mofizur. Rahman, Motoki Ueda, Takuji Hirose, Yoshihiro Ito

Peptide Science 2018, **2019**, in press.

Acknowledgments

First of all, I would like to express my deep gratefulness to **Dr. Yoshihiro ITO**, chief scientist in RIKEN, who gave me the opportunity to join his research team at RIKEN and supported me to get the financial support and adopted as JRA at RIKEN. I sincerely thank him for his esteemed supervision, continuous advices, valuable discussions, and reviewing the thesis from the initial to the end. I really appreciate his very generous support and cooperation for my family life in Japan. I am grateful to him.

I express my appreciative thanks to **Prof. Takuji HIROSE**, who supported me to pursue my doctoral study at Saitama University under his academic supervision. I am thankful for his enthusiastic support, continuous advices and encouragement. I express my gratitude to him for giving me the freedom to investigate the research areas that I found interesting. I really appreciate his endless support, his valuable time and efforts since I started my admission procedures until my graduation.

I would like to express my deep gratitude to my supervisor **Dr. Motoki UEDA** in RIKEN, who suggesting the points of this research and supporting me point by point at all stages of this work from the initial conception to the end of this work. My grateful thanks to him for everything he did for me during my study within three years: his endless support, kind patience, unlimited encouragement, very effective project meetings, everyday research discussions, and important advices. I strongly believe that a lot of knowledge and skills I gained under his esteemed supervision.

I would like to express my thanks and gratitude to the Doctoral Reviewers Committee: **Prof. Koji MATSUOKA**, **Assoc. Prof. Ken HATANO**, and **Assoc. Prof. Koichi KODAMA** for their valuable suggestions and very useful comments in my defense. I strongly believe that my thesis has been improved by the suggestions and discussion.

Concluding Remarks

I am especially thankful to **Dr. Siyoong SEO & Kon SON** for their very useful discussion and their kind help for TEM study and various assistance during initial experiment in lab. I sincerely thank **Dr. Nandakumar AVANASHIAPPAN** for his kind help for CD and NMR measurements as well as various assistance during synthetic works.

I am thankful to my colleagues: **Dr. Baiju G. NAIR, Dr. Jun AKIMOTO, Stefan MÜLLER**, and all members of **my lab mates** for their very friendly help, always encouragement and kind support during my research study in various ways.

I sincerely thank **Mrs. Akiko NOSE** and **Mrs. Kyoko YAMANAKA** for their very kind help for me from the first day that arrived in Japan until finishing my Doctoral study. I acknowledge **RIKEN JRA program** for giving me this chance to study in Japan under their financial support.

I would like to express my thanks to staff members of **Graduate School of Science and Engineering, Saitama University** for their kind help and cooperation during the progress of my admission and graduation steps. I acknowledge all the staff members of the **international affairs section** at **Saitama University** for their cooperation and kind support during my stay in Japan.

I am grateful to my Supervisors and Colleagues of Department of Pharmacy, Faculty of Science and Engineering, **Khulna University and Bangladesh University, Bangladesh** for their enthusiastic support, continuous advices, and encouragement.

A very deep appreciation is to **elder brother, my father, my sisters, and my brothers** for their constant encouragement and for their prayers for me at all the time.

I would like to express my gratitude to my second family **father, mother, sister, and brothers of my wife** for their constant support and their continuous encouragement.

Finally, my heartfelt thanks is to my wife *Santona* and my daughter *Nureen* who are the partner of my life and motivation of this work. My very deep gratitude is for their endless encouragement and support through this important stage in our life.

Rahman Md Mofizur

Graduate School of Science and Engineering,
Saitama University, JAPAN

Emergent Bioengineering Materials Research Team,
Center for Emergent Matter Science (CEMS), RIKEN, JAPAN

s16ds006@mail.saitama-u.ac.jp

md.mofizur.rahman@riken.jp

rmfi02@yahoo.com

2019. March